Combustion Bowl Heat Transfer Analysis in Diesel and PPC Engines

Fridriksson, Helgi

2013

Combustion Bowl Heat Transfer Analysis in Diesel and PPC Engines

LUND
UNIVERSITY

Helgi Fridriksson

AKADEMISK AVHANDLING/DOCTORAL DISSERTATION

för avläggande av teknologie doktorsexamen vid Tekniska Fakulteten, Lunds Universitet, kommer att offentligen försvaras tisdagen den 17:e december kl. 10:15 i hörsal B, M-huset, Ole Römers väg 1, Lund. Fakultetsopponent: Professor Morgan Heikal, Univesity of Brighton, UK.

by due permission of the Faculty of Engineering at Lund University, will be defended on Tuesday 17th of December at 10:15 a.m. in Lecture hall B in the M-building, Ole Römers väg 1, Lund. Faculty opponent: Professor Morgan Heikal, University of Brighton, UK.

Organization LUND UNIVERSITY Division of Heat Transfer Department of Energy Sciences Faculty of Engineering	Document name DOCTORAL DISSERTATION Date of issue 2013-12-17 Sponsoring organization Swedish Energy Agency Volvo Car Corporation
Author(s) Helgi Fridriksson	

Title and subtitle

Combustion Bowl Heat Transfer Analysis in Diesel and PC Engines

Abstract

This thesis concerns a numerical investigation on heat transfer in internal combustion engines, with the aim of increasing engine efficiency. The efficiency gains are to be extracted from reduced heat transfer losses, by increasing the knowledge on how the heat transfer process is affected by various hardware and operational parameters in the engine. The engines concerned are both conventional diesel engines and engines operated in partially premixed combustion mode. In the thesis, heat transfer results for these two engine modes are compared and discussed. In addition, evaluation of the engine performance and emissions is done in order to confirm that reduced heat losses contribute to increased efficiency.

The numerical investigation is based upon three-dimensional computational fluid dynamics simulations using RANS based models, where transport equations for turbulent reacting flows inside the engine cylinder are solved. The engine is represented by an engine segment model, where a single spray enclosure for the closed volume part of the cycle is simulated. This provides information on the compression, combustion and expansion part of the cycle, where the interaction between combustion and heat transfer are studied for the two combustion modes.

The results showed that heat transfer can be affected by both operational and geometrical parameters, while the results for emission values differed between the engine concepts. Changing the piston geometry in the engine lead to changes in the engine flow-field and, thereby, the amount of heat transfered from the engine cylinder. Another efficient tool for affecting engine heat transfer was the manipulation of the injection strategy. The results showed that with a favorable injection strategy, the high-temperature in-cylinder gases could be stratified so the engine walls would be sheltered from the high-temperature gases. This lead to a reduced temperature gradient in the near-wall region and reduced heat transfer. Other parameters that had an effect on engine heat transfer were inlet pressure and temperature values. These were optimized for optimal trade-off between engine heat transfer, engine performance and emission levels. Comparing the conventional diesel combustion concept and the partially premixed combustion concept, while moving towards adiabatic conditions, revealed that even though engine performance was improved for both combustion concepts, emission levels were quite different. Lower temperature during combustion in the PPC mode resulted in a more modest increase in emission levels, while conditions were moved towards adiabatic wall conditions.

Key words: Heat transfer, CFD, internal combustion engine, diesel, ppc

Classification system and/or index termes (if any):

Supplementary bibliographical information:		Language English
ISSN and key title: 0282-1990		ISBN 978-91-7473-752-3
Recipient's notes	Number of pages	Price
	Security classification	

Combustion Bowl Heat Transfer Analysis in Diesel and PPC Engines

Helgi Fridriksson

LUND
UNIVERSITY

Department of Energy Sciences
Faculty of Engineering

Thesis for the degree of Doctor of Philosophy in Engineering.

Division of Heat Transfer
Department of Energy Sciences
Faculty of Engineering
Lund University
Box 118
SE-221 00 LUND
SWEDEN

ISBN 978-91-7473-752-3 (Print)
ISBN 978-91-7473-753-0 (Pdf)
ISRN LUTMDN/TMHP-13/1099-SE
ISSN 0282-1990

Typeset in LaTeX
Printed by Tryckeriet i E-huset, Lund, Sweden, December 2013.

Populärvetenskaplig sammanfattning

Transporter är viktiga för ett fungerande samhälle, men samtidigt innehåller avgaserna från en förbränningsmotor farliga utsläpp som förorenar vår miljö. Kan vi på något sätt hindra att miljön blir förstörd av farliga utsläpp genom förbättrad motordesign?

Frågan om global uppvärmning har varit vid liv enda sedan IPCC (Intergovernmental Panel on Climate Change) grundades och Kyoto-protokollet infördes, vilket har lett till kännedom om växthusgaser och deras inverkan på jordens temperatur. Den diskussionen har tagit mycket tid och plats i dagens media och resulterat i en rad lagstiftningar angående tillåten mängd emissioner från bland annat förbränningsmotorer. Mängden farliga emissioner som bildas i en förbränningsmotor är starkt kopplad till både mängden bränsle som förbränns, samt gastemperaturen under förbränningsprocessen.

I en dieselmotor sugs atmosfärisk luft in till varje cylinder, ofta trycksatt med hjälp av en turbindriven kompressor. I cylindern komprimeras luften, innan bränslet sprutas in och självantänds på grund av det höga trycket och temperaturen. Under förbränningen frigörs värme när bränslet oxiderar och bildar förbränningsprodukter, t.ex. koldioxid (CO_2) och vatten (H_20). Under den termodynamiska cykeln omvandlas det frigjorda värmet till användbart mekaniskt arbete, som i sin tur driver, exempelvis, en bil framåt. Under cykelns gång uppstår det ett antal förluster, som, till stor del, inte går att återvinna. Traditionellt brukar man uppskatta att ungefär en tredjedel av bränsleenergin omvandlas till mekaniskt arbete, medan resten av energin delas nästan jämnt mellan en ren värmeförlust genom cylinderns väggar och avgasvärme. I nutida motorer har fördelningen av bränsleenergin blivit mer fördelaktig tack vare förbättrad motordesign, vilket innebär snålare motorer och lägre koldioxidutsläpp. Fortfarande försvinner mer än hälften av bränsleenergin i rena värmeförluster, vilket gör att bättre kunskap om värmetransporter i motorn och dessas inverkan på emissionsbildning är av yttersta vikt för framtida motorer.

Den här avhandlingen handlar om en numerisk studie av värmetransporter i dieselmotorer, där motorn har körts med två olika förbränningskoncept. Det ena är konventionell dieselförbränning och det andra är ett nytt förbränningskoncept som heter Partially-Premixed Combustion (PPC), vilket betyder partiellt förblandad förbränning. I PPC-konceptet frigörs värmet från förbränningen normalt under en kortare period än vid konventionell dieselförbränning. Dessutom är den maximala temperaturen under förbränningsfasen inte lika hög som i dieselförbränning, på grund av ändrad strategi för insprutning av bränsle och större mängd inerta gaser. Detta har gjort att PPC-förbränning har visat lägre värden på värmeförluster, samtidigt som verkningsgraden för motorn har stigit och mängden farliga emissioner har minskat. Detta har visats i encylindriga motorexperiment vid Lunds Universitet. Forskningen i denna avhandling har varit

inriktad mot att återskapa motorexperiment med tre-dimensionella datorsimuleringar, för att bättre kunna studera värmetransporter. Dessa studier involverar dieselmotorer för både personbilar och lastvagnar, såväl som lastvagnsmotorer med PPC förbränning.

Resultaten visar att temperaturfördelningen för gaserna inuti motorcylindern kan påverkas av hur och när bränslet sprutas in i cylindern. Genom att påverka introduktionen av bränslet i cylindern var det möjligt att hålla gaserna nära väggarna kallare, vilket gjorde att energin inte försvann lika snabbt ut genom motorns väggar. En annan parameter som avgjorde hur mycket energi som transporterades genom väggarna var själva utformningen av förbränningsrummet. Hur förbränningsrummet ser ut kommer att ha inverkan på hela flödesfältet i motorn och om man kan utforma flödesfältet så att flödeshastigheterna nära väggarna blir lägre, så blir energitransporten genom väggarna lägre. Detta innebär att värmetransporterna i motorn kan påverkas genom en lämplig kombination av insprutningsstrategi och geometri.

Abstract

This thesis concerns a numerical investigation on heat transfer in internal combustion engines, with the aim of increasing engine efficiency. The efficiency gains are to be extracted from reduced heat transfer losses, by increasing the knowledge on how the heat transfer process is affected by various hardware and operational parameters in the engine. The engines concerned are both conventional diesel engines and engines operated in partially premixed combustion mode. In the thesis, heat transfer results for these two engine modes are compared and discussed. In addition, evaluation of the engine performance and emissions is done in order to confirm that reduced heat losses contribute to increased efficiency.

The numerical investigation is based upon three-dimensional computational fluid dynamics simulations using RANS based models, where transport equations for turbulent reacting flows inside the engine cylinder are solved. The engine is represented by an engine segment model, where a single spray enclosure for the closed volume part of the cycle is simulated. This provides information on the compression, combustion and expansion part of the cycle, where the interaction between combustion and heat transfer are studied for the two combustion modes.

The results showed that heat transfer can be affected by both operational and geometrical parameters, while the results for emission values differed between the engine concepts. Changing the piston geometry in the engine lead to changes in the engine flow-field and, thereby, the amount of heat transfered from the engine cylinder. Another efficient tool for affecting engine heat transfer was the manipulation of the injection strategy. A study showed that with a favorable injection strategy, the high-temperature in-cylinder gases could be stratified so the engine walls would be sheltered from the high-temperature gases. This lead to a reduced temperature gradient in the near-wall region and reduced heat transfer. Other parameters that had an effect on engine heat transfer were inlet pressure and temperature values. These were optimized for optimal trade-off between engine heat transfer, engine performance and emission levels. Comparing the conventional diesel combustion concept and the partially premixed combustion concept, while moving towards adiabatic conditions, revealed that even though engine performance was improved for both combustion concepts, emission levels were quite different. Lower temperature during combustion in the PPC mode resulted in a more modest increase in emission levels, while conditions were moved towards adiabatic wall conditions.

Acknowledgements

Throughout my journey as a PhD student I have had the pleasure to work with extremely competent people within the Department of Energy Sciences at Lund University, without whom this work would not have seen the light of day.

To my main supervisor, Professor Bengt Sundén, I would like to thank you for the opportunity to pursue my academic career within the field of heat transfer. Your guidance and experience within the field is valuable and I am very grateful to have been a part of your research team. My co-supervisors, Dr. Shahrokh Hajireza and associate Professor Martin Tunér, have also inspired me with valuable discussions on methods and results during my simulation work. Martin, I would also like to thank you for introducing me to the wonderful world of internal combustion engines, as well as the many hours spent on making sense of my results. In addition, I would like to thank Professor Öivind Andersson for his valuable input, both regarding the work on design of experiments and also during my work with the light duty engine.

I would like to express my gratitude to my wonderful co-workers at the Division of Heat Transfer for enjoyable moments during my stay at the department. I hope to see as many of you in the future and would welcome further co-operation.

To my contacts at Scania, Eric Baudoin and Johan Forss, as well as my contacts at Volvo Cars, Håkan Persson, Mattias Ljungqvist and Joop Somhorst, I really appreciate your input, both regarding engine specific details and general discussions on engine development.

To my dear wife Berglind and my children Birta, Daniel and Hilmar, I am forever grateful for the all the support and encouragement you have given me throughout this process. I know it has not been easy, but you always managed to push me forwards and motivate me. To my parents, Friðrik and Helga, my sister Bryndís and brother Hlynur, I am very grateful for all the support you have given me throughout my entire studies.

This work has been made possible by financing from the Swedish Energy Agency as well as the Volvo Car Corporation. The computational software used during this thesis work has been graciously provided by AVL List GMBH in Austria, which is gratefully acknowledged. A part of the simulation work has been done using computer cluster at Lund University, made possible by the Swedish National Infrastructure for Computing (SNIC).

List of publications

The thesis is based on the following papers, which will be referenced by roman numericals in the body text of the thesis. The papers are appended in the oder listed below.

I **H. Fridriksson**, B. Sundén, S. Hajireza, *A Theoretical Study on the Heat Transfer Process in Diesel Engines*, Advanced Computational Methods and Experiments in Heat Transfer XI, 177-188, 2010.

II **H. Fridriksson**, B. Sundén, S. Hajireza, M. Tunér, *CFD Investigation of Heat Transfer in a Diesel Engine with Diesel and PPC Combustion Modes*, JSAE/SAE International Powertrains, Fuels & Lubricants, Kyoto, Japan, 2011-01-1838, 2011.

III **H. Fridriksson**, S. Hajireza, M. Tunér, B. Sundén, *A CFD Investigation of Heat Transfer in a Diesel Fueled PPC Engine Applying Design of Experiments*, Proceedings of the ASME International Combustion Engine Division Fall Technical Conference, Vancouver, BC, Canada, ICEF2012-92059, 2012.

IV **H. Fridriksson**, S. Hajireza, M. Tunér, B. Sundén, *CFD Investigation on Injection Strategy and Gasoline Quality Impact on In-Cylinder Temperature Distribution*, 11th International Conference on Engine Vehicles, Capri, Italy, 2013-24-0009, 2013.

V **H. Fridriksson**, M. Tunér, Ö. Andersson, B. Sundén, M. Ljungqvist, H. Persson, *Effect of Piston Bowl Shape and Swirl Ratio on Engine Heat Transfer in a Light-Duty Diesel Engine*, Submitted to the SAE World Congress 2014, Detroit, USA.

Author contribution
For papers I-V, the thesis author was responsible for the computational model, running simulations, analysis of the results and writing the papers.

Nomenclature

Latin letters

A	Area [m^2]
B	Engine bore [m]
C	Model constant (various models)
c_p	Specific heat
c	Species concentration
f	Elliptic relaxation function
H	Total enthalpy
h_c	Convective heat transfer coefficient [W/m^2K]
k	Turbulent kinetic energy, reaction rate constant
p	Pressure [bar]
$\dot{q}$	Convective heat flux per unit area [W/m^2]
$\dot{Q}$	Convective wall heat flux [W]
$\dot{r}_{fu}$	Reaction rate of fuel in the eddy break-up model
S	Source term
$\overline{S}_p$	Mean piston velocity
T	Temperature [K]
t	Time [s]
u	Velocity
V	Volume
V_d	Displacement volume
y_i	Mass fraction of species i

Greek letters

α_s	Scaling factor in global heat transfer models
β	Velocity scaling in the Hohenberg model
δ_{ij}	Kronecker delta
ϵ	Turbulence dissipation
ζ	Velocity scale ratio
λ	Thermal conductivity
μ	Dynamic viscosity
ρ	Density
σ	Stefan-Boltzmann constant
σ_t	Turbulent Prandtl number
τ	Viscous stress, chemical reaction time scale
Φ	Equivalence ratio [-]
ϕ_s	Soot mass fraction
ω	Angular velocity

Chemical

CO	Carbon monoxide
CO_2	Carbon dioxide
H_2O	Water
N	Nitrogen
NO_x	Nitric oxides
O	Oxygen

Acronyms & Abbreviations

ATDC	After Top Dead Center
BTDC	Before Top Dead Center
CAD	Crank angle degree
CFD	Computational Fluid Dynamics
CI	Compression Ignition
DoE	Design of experiments
ECFM-3Z	3 Zone Extended Coherent Flame Model
EGR	Exhaust Gas Recirculation
EVM	Eddy Viscosity Model
EVO	Exhaust valve opening
GA	Genetic Algorithm
HCCI	Homogeneous charge compression ignition
HD	Heavy duty
IC	Internal Combustion
IVC	Inlet valve closing
LHR	Low Heat Rejection
LD	Light duty
LTC	Low Temperature Combustion
MEP	Mean Effective Pressure
PPC	Partially Premixed Combustion
Pr	Laminar Prandtl number
RANS	Reynolds Average Navier-Stokes
Re	Reynolds number
SI	Spark ignited
TDC	Top dead center

Contents

List of Figures

CHAPTER 1

Introduction

Modern society is highly dependent on energy consumption in all forms; heavy industry, service, household and transportation. According to a report from the Swedish Energy Agency, around a third of the country's total energy usage is from the transport sector [1], where the internal combustion (IC) engine is a commonly used energy conversion device. Figure 1.1 shows that since the 1970's, the energy consumption from the transport sector has almost doubled, but after 2005 there has been a stagnation of this increase. There are a few drivers behind

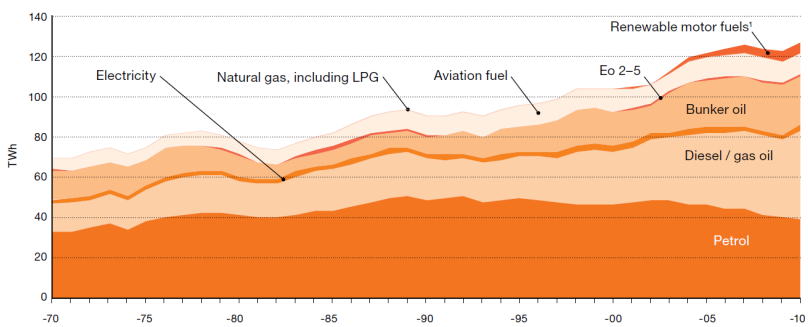

Figure 1.1: *Energy usage in the Swedish transport sector [1].*

this stagnation, one of which is increased focus on public transport, while others have been more directed towards improving current internal combustion engine designs. Since the creation of the Intergovernmental Panel on Climate Change (IPCC), environmental awareness has increased, which has lead to toughened legislation on engine emissions. The latest European emission standard, Euro 6 (2014), restricts emission levels to only a fraction of the levels allowed in the first Euro 1 standard (1992), as shown in Table 1.1.

Table 1.1: *Emission standards for heavy-duty diesel engines [2]*

Stage	Year	CO	HC	NO_x	PM	PN	Smoke
			g/kWh			$1/kWh$	$1/m$
Euro 1	1992	4.5	1.1	8.0	0.36		
Euro 2	1996	4.0	1.1	7.0	0.25		0.15
Euro 3	2000	2.1	0.66	5.0	0.10		0.8
Euro 4	2005	1.5	0.46	3.5	0.02		0.5
Euro 5	2008	1.5	0.46	2.0	0.02		0.5
Euro 6	2013	1.5	0.13	0.4	0.01	8.0×10^{11}	

CO_2 emissions are, however, not among the emissions regulated by the Euro standards. In the year 2006, the Swedish government introduced a vehicle tax based on the vehicle's carbon dioxide (CO_2) emissions, instead of only its weight, as previously. This, along with increased oil prices is a large driver for an improved engine design, in terms of engine efficiency as well as emissions.

1.1 Importance of engine heat transfer

Traditionally, the work output of a IC engine has been divided into three outgoing energy flows; work, exhaust enthalpy and heat transfer, yielding a break efficiency in the low-to-mid 30's (%) [3]. A spark-ignited (SI) engine, commonly known as a gasoline engine, would have an efficiency in that region, but a compression ignition (CI) engine, diesel, would be slightly more efficient, due to higher compression ratios and lower throttling losses. A modern diesel engine can have a break efficiency in the low 40's (%). This means that if the ratio between work, exhaust enthalpy and heat transfer was to be shifted in favor of the work output, the engine efficiency, and consequently the fuel consumption and CO_2 emissions, would improve.

When the IC engine is studied in more detail, it can be noted that the engine can be divided into a series of interacting subsystems. Borman & Nishiwaki [4] list six subsystems within a diesel engine, each with their own level of complexity

when it comes to the evaluation of flow patterns and heat transfer. In each of the subsystems, heat transfer plays a significant role for the performance of the engine. During the intake stroke higher temperatures will decrease the volumetric efficiency, indicating that less amount of fresh air will be used in the cycle, and thereby slightly lowering the overall performance of the engine. During compression the peak pressure is affected by the heat transfer mechanisms in the engine cylinder. However, the largest and most significant contribution from the heat transfer process in a diesel engine is experienced during the combustion and expansion. Then, the convective and radiative heat transfer from the gases and particles in the cylinder are combined with the conductive heat transfer through the cylinder head, walls and piston to the cooling passages and lubricating oil [3, 4]. Due to the transient behavior of the fluid motion inside the engine cylinder, the heat flux to the solid components of the cylinder may vary from 0 to as much as 10 MW/m^2 during the span of a few milliseconds. Furthermore, two points on the cylinder wall, separated only by one centimeter, may experience the same difference in heat flux, introducing large thermal stresses in the solid components [4, 5]. Heat transfer is also important for spray and combustion related phenomena, such as droplet evaporation, auto-ignition and flame-wall interaction [6–8].

Figure 1.2 shows the energy cascade from fuel energy down to the power output, to scale, for a heavy duty diesel engine. The figure shows all the major losses within the engine cylinder, given in MEP (Mean Effective Pressure). The figure indicates that the research areas of interest for increased engine efficiency are engine heat transfer and exhaust losses, as they are dominant in this figure. On the other hand, a conversion of heat into work in a thermodynamic cycle, without the exchange of heat with the environment, is in violation of the Kelvin-Planck statement of the second law of thermodynamics [9]. Therefore, it is impossible to exclude heat losses or exhaust losses from the engine cycle. However, it should be possible to obtain a reduction in the heat losses, in order to increase the engine efficiency further.

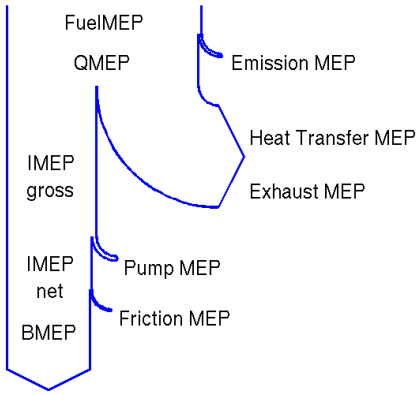

Figure 1.2: *Energy cascade from fuel energy to the engine's power output. FuelMEP = Fuel energy input, BMEP = Work output.*

1.2 Research objectives

There are various ways to go about engine heat transfer studies. The main core of this thesis work is focused on two main questions:

- How is engine heat transfer affected by engine conditions?
- How do the engine hardware parameters affect engine heat transfer?

The first question is focused on engine conditions, meaning the engine load and conditions of the inlet gases. These parameters surely have an effect on the engine performance, but what about the in-cylinder heat transfer?

The second question is more related to how the engine construction itself can be adjusted to minimize heat losses. Within the scope of the engine construction one will find parameters related to the injector properties, intake port alignment and combustion chamber geometry, to name a few. These are also bound to influence heat transfer, as their effects on engine performance and emissions is quite well documented.

The objectives in the presented work were two-fold. First, all current information on available sub-models needed to be collected in order to construct a working three-dimensional CFD model for heat transfer predictions. Second, use the model to make variations in the most interesting heat transfer related parameters and investigate how the heat transfer process within a diesel engine can be influenced. The main idea was to gain more knowledge on engine heat transfer to be able to eventually limit engine heat losses for further gain in work output and engine efficiency.

1.3 Methodology

In order to carry out heat transfer analysis of a diesel engine, a working model needs to be available. In this work the engine modeling has been focused on the closed volume part of the engine, from the time of inlet valve closing (IVC) to the time of exhaust valve opening (EVO). During this period, the heat fluxes from the gases to the cylinder walls are largest and the largest heat loss reduction can be achieved. The choice of engine modeled in the work has been dictated on the data available from the engine labs at Lund University, so a large portion of the work has been carried out using geometries from the truck manufacturer Scania, in Södertälje. Two of their truck engines, the 12 liter D12 engine and their 13 liter D13 engine, have been modeled in the papers presented, with different combustion modes. These different combustion modes are the conventional diesel combustion and the newer concept of partially-premixed combustion, which will be described in Chapter 2. Additionally, a light-duty car engine from the Volvo Car Corporation has been modeled, along with a medium-duty AVL research engine, both modeled with diesel combustion.

1.4 Thesis outline

In Chapter 2, a background on the combustion concepts used in this thesis work is given. In the chapter, the present heat transfer modes inside a internal combustion engine are discussed, along with the available modeling approaches for engine heat transfer, for both of the combustion concepts used in the thesis work. Chapter 3 gives an overview of the CFD model used in the thesis work, along with possible alternatives for some of the sub-models in the simulation work. The turbulence modeling alternatives are discussed along with spray, combustion and emissions modeling. Different temperature wall function formulations are also listed and compared in the chapter. The engines that were used for the simulation work are presented in Chapter 4. Four different engines were modeled, two heavy-duty (HD) engines, one light-duty (LD) engine and one medium-duty (MD) engine. Chapter 5 summarizes the most important results from the papers that make up this doctoral thesis and these results are discussed in the context of what they mean for future engine development. For more detailed information about specific results, the reader is referred to the attached papers. In Chapter 6, concluding remarks are made along with comments on the future outlook of the field of heat transfer modeling in diesel and ppc engines.

CHAPTER 2

Background

In this thesis two different combustion modes for a compression ignition engine are studied; conventional diesel combustion and partially-premixed combustion (PPC). The following sections provide a brief description of the main characteristics of these two combustion modes and their main difference with regards to heat transfer.

2.1 Diesel combustion

In compression-ignition engines, air from the intake is often compressed before being introduced to the engine cylinder. The air is compressed further in the cylinder, until the top-dead center position of the piston. Liquid fuel is injected around the desired time of combustion and, depending on the compression ratio and the fuel properties, the delay from injection to ignition may vary. Load variation is controlled primarily by the amount of fuel injected each cycle, while the air flow remains relatively unchanged [3]. A conventional diesel combustion is a spray driven combustion process, that consists primarily of a diffusion flame, meaning that air and fuel only mixes at the reaction zone. In 1997, John Dec presented a conceptual model on how a diffusion flame looks in a diesel engine, based on laser-sheet imaging [10]. This conceptual model is portrayed in Fig. 2.1 and shows that the liquid fuel travels a certain amount of length (liquid penetration length), before being vaporized and mixed with the surrounding air. The

flame is stabilized at a certain distance (lift-off length) from the injector hole. The model also shows in which regions of the flame the most common diesel combustion emissions, NO_x and soot, are formed and this conceptual model has served as a basis for a number of sub-models being used in computation today.

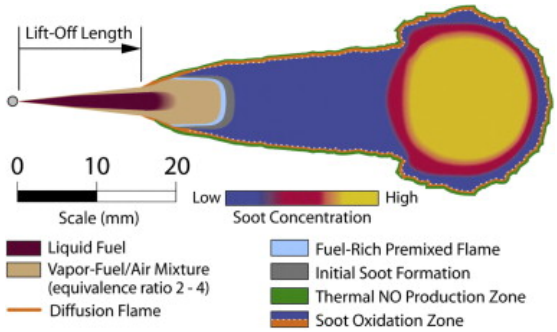

Figure 2.1: *Conceptual model of a diesel flame [10].*

Most emissions in diesel engines are dependent on the ratio of fuel and air during combustion, as in a fuel rich combustion larger amounts of unburned hydrocarbons (UHC) and carbon monoxide (CO) are present in the exhaust. There are also emissions that are more strongly temperature dependent, such as NO_x and soot. Kamimoto and Bae [11] introduced a $\Phi - T$ map, shown in Fig. 2.2, which demonstrated the temperature dependence of NO_x and soot emissions. According to the figure, soot emissions are formed at fuel-rich conditions and temperatures between 1500 and 2600 K, while NO_x emissions are formed at higher temperatures and fuel-lean conditions. This figure can be used to highlight that a certain control of the combustion temperature must be in place, in order to keep emission levels low. It should also be mentioned that the location of the soot and NO_x production zones is dependent on the chemical composition of the gases in the cylinder, meaning that they are dependent on the fuel and chemical composition of the intake gas mixture. Recently, it has become more common to make use of cooled exhaust gases (EGR) in order to dilute the incoming air-charge. This has resulted in an effective way to reduce peak combustion temperature and control the formation of temperature dependent emissions. A problem that has risen when introducing these high levels of EGR, is when predicting the auto-ignition process and the combustion phasing using combustion models derived for diesel combustion, without EGR.

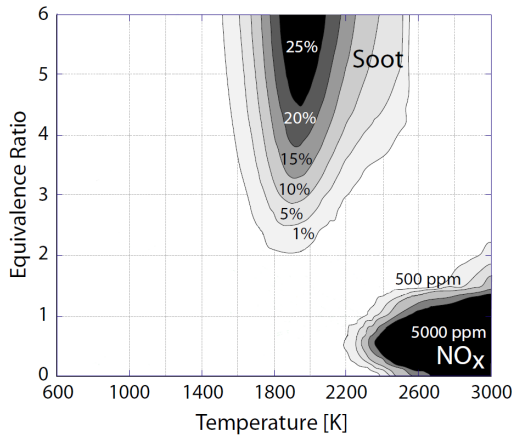

Figure 2.2: $\Phi - T$ *map constructed by Kamimoto and Bae [11].*

2.2 Partially premixed combustion (PPC)

In the pursuit of a combustion concept which provides a high efficiency output, together with low emission levels, the concept of *low-temperature combustion* (LTC) has provided a pathway towards a solution. LTC engines are a group of engines that are based on lean- or diluted mixtures of fuel and air resulting in lower peak temperatures during combustion and were first introduced with the 2-stroke *ATAC* engine, presented by Onishi *et al.* [12]. This lean-burn autoignition concept was revived in the late 90's and became better known as *HCCI*, or *Homogeneous Charge Compression Ignition*, where a homogeneous charge of fuel and air is ignited by compression, as described in [13, 14]. Even though HCCI has been shown to have extremely good characteristics in terms of thermodynamic efficiency together with low emissions, there is problem with combustion control, due to the fact that HCCI combustion is entirely controlled by chemical kinetics. This leaves HCCI engines sensitive to in-cylinder pressure and temperature, as well as fuel reactivity and equivalence ratio. In order to overcome these problems, a concept called *Partially premixed combustion*, or *PPC* has been introduced. With PPC, combustion can be controlled by the fuel injection strategy as well as fuel and EGR levels. Compared to HCCI, the load range for PPC is considerably wider, without compromising the performance of the engine. The two concept share the property of higher thermodynamic efficiency, compared to traditional SI and CI engines, together with low emission levels [13–15].

The PPC concept, as described by Manente [15], is an intermediate process between HCCI combustion, using a fully premixed charge, and conventional diesel combustion, where fuel is injected while combustion is occurring. Fuel is thereby injected in the compression stroke to allow for some mixing with air before the start of combustion. According to Manente [15], all of the fuel should be injected before the start of combustion, but not too early in order to prevent violent combustion with high peak pressure, peak pressure rates and pressure oscillations. This fuel injection strategy is combined with high levels of EGR in order to dilute the air/fuel mixture and to assure low temperature combustion. This strategy has shown to provide high efficiency and extremely low emissions for a wide load range of a heavy duty diesel engine [16]. Recently, there has been a considerable amount of research conducted on partially premixed combustion, both experimentally and numerically. Single cylinder experiments are being conducted with promising results at Lund University [17, 18], where numerical evaluation of the concept are also being carried out [19–24]. As a result from this research, one explanation to the increased efficiency of the PPC concept over conventional diesel, is reduced heat losses. Tuner *et al.* [24], showed a comparison between the energy flows in a six-cylinder heavy duty engine operated in conventional diesel and PPC modes. A part of the results is summarized in Fig. 2.3, where the losses in the two engine modes are compared. The figure shows that heat transfer losses are reduced from 12% of the fuel energy, in the diesel case, to only 5% of the fuel energy, in the PPC case. At the same time, pumping losses increase from 1 to 3%, due to higher turbo-charging. With the exhaust energy unchanged, the indicated break efficiency is increased by 5 percentage points.

Other new LTC concept have been introduced by other research groups and out of those, the most promising ones are *Premixed Charge Compression ignition*, or *PCCI* for short, and *Reactivity Controlled Compression Ignition*, or *RCCI* for short. The largest research effort on these concepts is being overseen by the University of Wisconsin, in the US. These concepts have both been used with a dual-fuel strategy, to demonstrate high efficiency together with low emission levels, over a wide load range [25–29]. A conceptual model, corresponding to John Dec's diesel spray model (Fig. 2.1), has been created for low temperature combustion concepts, like PPC, at Sandia National Laboratories in California. The model, shown in Fig. 2.4, has been published by Musculus *et al.*[30] and it clearly demonstrates how fundamentally different the combustion process in LTC concepts is, compared to conventional diesel combustion. In the figure LTC combustion (on the right) is compared to conventional diesel combustion (on the left), to highlight the major differences between the combustion concepts. This model can be used to further the understanding of LTC behavior, specially regarding how and where emissions are produced during the combustion process.

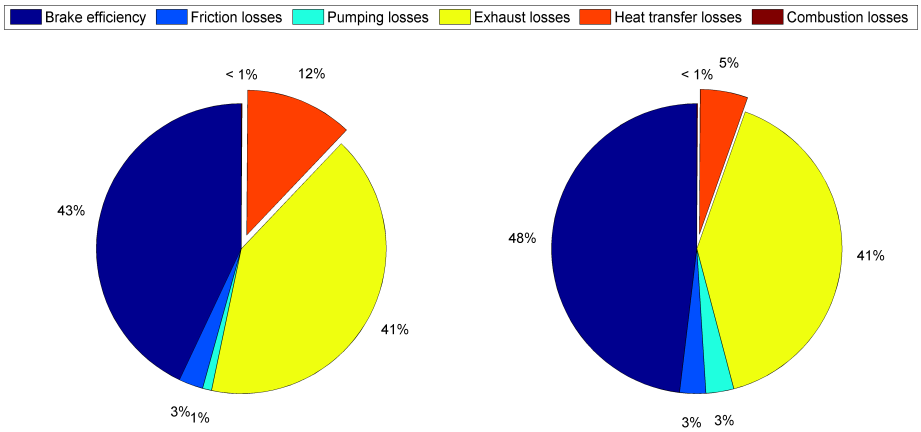

(a) *Diesel combustion* **(b)** *Partially premixed combustion*

Figure 2.3: *Energy flow in the two combustion modes, recreated from [24].*

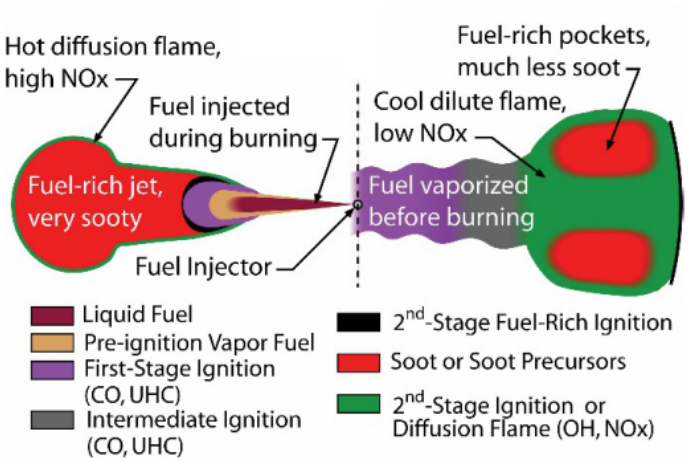

Figure 2.4: *Left side: Conceptual diesel combustion model.*
Right side: LTC conceptual model [30].

2.3 Heat transfer in IC engines

During one cycle in an internal combustion engine, all principle modes of heat transfer are present. The contribution of each mode is dependent on the engine operation condition, and chemical composition of the in-cylinder gases. The following section gives an introduction to each principle mode of heat transfer.

2.3.1 Conduction heat transfer

When a body is exposed to a temperature gradient, energy is transferred from the high-temperature region to the low-temperature region. This transfer is a result of molecular diffusion and particle collision and is commonly known as *conduction heat transfer*, which is governed by Fourier's law

$$\dot{Q} = -\lambda A \nabla T \tag{2.1}$$

where $\dot{Q}$ is the heat flux per unit time and λ is the thermal conductivity. This is the governing heat transfer mode for all solid parts of the engine; cylinder head, walls and piston. Heat transfer between solid parts is also governed by this heat transfer mode, as heat transfer from piston rings to the cylinder wall.

2.3.2 Convection heat transfer

When heat is transported by means of fluid motion, as well as between a fluid and a solid surface in relative motion, the process is called *convection heat transfer*. There are two main convection transport modes; natural convection (by means of gravitational forces) and forced convection (by means of additional forces). The convective heat transfer in engines is governed by forced convection of the turbulent flow field. If the engine is divided into three parts, the first part being the induction of air, second the cylinder itself and third the exhaust port and manifold, then the convective heat transfer is quite different between these parts. In the induction of air, heat is predominantly transferred from the engine walls to the incoming air, heating the air-charge before entering the cylinder. In the cylinder there is additional heating during the compression stroke, which is changed to cooling of the in-cylinder gases before combustion is started. Then heat is transferred from the gases to the cylinder walls by means of convection, through the walls by conduction and finally to the coolant by forced convection. In the exhaust port and manifold, due to high exhaust temperatures, heat is transferred from the air stream to the walls. Finally heat from the engine block is transferred to the surrounding, to a large extent, by convection. Convective transport between a solid surface and a fluid in motion is governed by Newton's law of cooling

$$\dot{Q} = h_c A (T - T_w) \tag{2.2}$$

where h_c is the convective heat transfer coefficient, which is dependent on the Reynolds- and Prandtl numbers, and A is the cross-sectional surface area of the heat transfer surface. T and T_w are the fluid- and wall temperatures, respectively.

2.3.3 Radiant heat transfer

Heat transfer in form of electromagnetic waves is commonly known as *thermal radiation*. In an internal combustion engine, heat is transferred by thermal radiation from the hot combustion gases and flame region to the engine walls, due to the large temperature difference. This process is governed by emission and absorption of electromagnetic waves, at wavelengths where energy is transformed into thermal energy within the visible and infrared ranges. The amount of heat transferred by thermal radiation varies between engine concepts and operational modes, being at its maximal magnitude in highly sooting, high temperature diesel combustion engines. Additionally, all external surfaces of significant temperature will not only exchange heat with the surroundings via convective heat transfer, but also via radiant heat transfer. The heat flux between two ideal radiators (black bodies) at temperatures T_1 and T_2, is given by

$$\dot{Q} = \sigma A(T_1^4 - T_2^4) \tag{2.3}$$

where the proportionality constant, σ, is called the Stefan-Boltzmann constant, having a value of 5.67×10^{-8} W/m$^2 \cdot$K^4. A ”black” surface absorbs and emits thermal energy equally well at all wavelengths, while non-black surfaces have a comparably lower emissivity of thermal energy. The surfaces and gases in real engine conditions do not behave as a blackbody, which introduces the need for adjustments when estimating the contribution from thermal radiation in engines. In modern engines, aside from highly sooting diesel engines, the contribution from thermal radiation is considered to be quite small in relations to the convective heat transfer. Additionally, adding thermal radiation to the already complex combustion system would translate into a considerable increase in computational effort within multi-dimensional modeling. For these reasons, radiant heat transfer is often omitted in multi-dimensional heat transfer analysis of IC engine cylinders. However, the contributions of thermal radiation can not be neglected when estimating the heat transfer between an IC engine and its surroundings.

2.4 Heat transfer modeling approaches

The importance of heat transfer in IC engines, and its effect on engine performance has been known from the beginning of engine research. However, heat transfer in IC engines is by many considered to be one of the most challenging applications within heat transfer, so no detailed solution of the problem is verified. Borman & Nishiwaki provided a comprehensive review of internal combustion engine heat transfer in 1987 [4], where the available experimental and modeling approaches of the time were highlighted. From their review, modeling approaches to engine heat transfer were divided into five main groups:

- Global thermodynamic models
- Zonal thermodynamic models
- One-dimensional analytical and numerical fluid-dynamics models
- Multidimensional numerical fluid-dynamics models (CFD)
- Radiant heat-transfer models

The zonal models, where the cylinder is divided into a number of smaller zones, each with their own temperature history and heat transfer coefficient, are not so commonly used in modern heat transfer estimations. They are from time to time being used coupled to one-dimensional fluid dynamics models, to get a better representation of the heat transfer process in the engine, compared to the global models, which only consider the cylinder to be a single zone.

2.4.1 Global models

In the global models, the in-cylinder convective heat transfer is assumed to follow Newton's law of cooling, as shown in Eq. (2.2), with a single heat transfer coefficient h to represent the entire inside surface of the cylinder. In some cases the combustion chamber surface is divided into a number of surfaces (N), each of a certain area (A_i). Then Eq. (2.2) can be re-written as

$$\dot{q} = \frac{1}{A} \sum_{i}^{N} h A_i (T - T_{w,i}) \tag{2.4}$$

where A is the total surface of the combustion chamber. The objective of the global models is to obtain an expression for the heat transfer coefficient in order to estimate the resulting heat flux to the engine walls. Since the early days of IC engine development, experimental data has been used for analysis and further development of engine design. In the early 20th century, several researchers focused their experimental studies on heat transfer in IC engines, in order to provide correlations to predict the gas-side convective heat transfer coefficient.

The first models were purely empirical models and in 1923, Nusselt proposed a model based on experiments on a spherical bomb [31]. His correlation, which contained both convective and radiant heat transfer, was a function of mean piston speed, pressure, gas- and wall temperatures as well as the emissivities of gas and wall. Although intended for time average heat flux predictions, this correlation has been more widely used to predict instantaneous heat fluxes. Another early correlation was proposed by Eichelberg in 1939 [32]. This correlation was based on experiments on a naturally-aspirated diesel engine and was given as a function of the mean piston speed, pressure and temperature.

Following the work of Nusselt and Eichelberg, other researchers turned to the use of similarity laws of steady turbulent heat transfer. The most widely known correlations of that form are those of Annand & Ma [33], Woschni [34] and Hohenberg [35]. The correlation proposed by Annand & Ma included a radiant term as well as a term including the angular velocity of the crank shaft. The resulting expression for the gas-side heat transfer coefficient is given in Eq. (2.5).

$$h_{\text{Annand\&Ma}} = \frac{\lambda}{B} Re^{0.7} \left(0.12 + \frac{0.12}{\omega (T - T_w)} \frac{dT}{dt} \right) \tag{2.5}$$

Woschni's proposal was based on heat balance instead of surface wall temperatures and also included a variable for the mean gas velocity in the cylinder, as well as the mean piston speed. Woschni's formulation for the gas-side heat transfer coefficient is provided in Eq. (2.6).

$$h_{\text{Woschni}} = \alpha_s B^{-0.2} p^{0.8} T^{-0.55} \left[C_1 \overline{S}_p + C_2 \frac{V_d T_1}{p_1 V_1} (p - p_0) \right]^{0.8} \tag{2.6}$$

Hohenberg proposed a formulation similar to Woschni's formulation, including the instantaneous cylinder volume. He also modified the exponent of the temperature term and slightly modified the gas velocity estimation.

$$h_{\text{Hohenberg}} = \alpha_s \, V^{-0.06} p^{0.8} T^{-0.4} (\overline{S}_p + \beta)^{0.8} \tag{2.7}$$

More recent attempts have been made to contribute with new global correlations for the instantaneous heat transfer coefficient for diesel and SI engines [36, 37]. These correlations have usually been produced from experimental work validated to a specific engine or combustion type. Furthermore, correlations have been introduced for heat transfer in other parts of the engine, like Depick and Assanis's correlation for heat transfer in intake and exhaust flows [38]. Even though many authors have proposed their own global heat transfer models, the Woschni model is still the most famous and widely used model for diesel engines.

Following the introduction of the low temperature combustion concepts, the need for new heat transfer correlation has risen. Some researchers have provided

alternative heat transfer correlations for these low temperature combustion engines, mostly HCCI engines, as Chang *et al.* [39]. Soyhan *et al.* published a review article in 2009 [40], where the most common correlations for diesel combustion engines were examined for HCCI combustion. The results were that, even though the Woschni model is the most widely used model for diesel engines, the Hohenberg model showed the best performance of the "standard" correlations for HCCI combustion.

These global heat transfer models are most often used for heat transfer estimation in one-dimensional gas exchange codes, where the engine system is simulated, as exemplified by [41]. Another application area of these models is heat release analysis, where the compensation of heat losses to the apparent heat release from combustion is made using these types of models. Within that application area, the Woschni model is dominating over other existing models for diesel combustion engines.

2.4.2 Multidimensional models

Recently the use of multidimensional models, more specifically computational fluid dynamics (CFD) codes, for engine simulations has increased. In these multidimensional models the engine geometry is resolved in two or three dimensions, with a finite number of computational cells, either for steady state or transient calculations. In the early days of multidimensional modeling, the field was dominated by finite element calculations for temperature distribution and thermal stress estimation in the solid parts of the engine, as shown in [42–45]. More recently the use of finite volume based codes has allowed for simulations of the flow motions of the gases in the cylinder, along with the temperature distribution in the gases and the convective heat transfer to the solid parts [46, 47].

The main advantage with CFD simulations is that a successful simulation can provide values for any parameter at any location in the engine, where engine experiments may be limited by accessibility. Furthermore, during an engine experiment, not all physical properties can be measured, like the concentration of individual species within the cylinder during combustion and the three-dimensional temperature distribution. The simulations can even be carried out for extreme operating conditions, which is usually not an option for experimental work. Performing CFD simulations in engines has, however, always been a difficult task because the level of complexity is relatively high. This applies both for the geometry, which not only contains moving parts but also contains areas that need extremely fine grid resolutions, and the physical processes that occur in the engine, such as turbulent flow, fuel spray injection and combustion. Giving a fair representation of both the geometry and the physics in the engine will result

in a high resolution both in time and space. This is not often feasible for engine design work, because a significant amount of time will be spent on computational mesh generation and simulations. For this reason simplifications, both for the geometry and physics, are usually made to save both time and effort. This calls for the use of sub-models which represent the physical behavior of the processes in the engine cylinder, such as turbulence, spray behavior and combustion.

The development of CFD models for diesel engine application is a constantly evolving process. Reitz and Rutland [48] list a few of the models needed in order to successfully simulate a diesel engine cycle, as well as their development until 1995. Since then, there have been vast improvements, such as the further formulation of temperature wall functions [49] and near wall treatment for turbulence in combination with conjugate heat transfer [50]. Spray and combustion models have also seen great progress in recent years.

Multidimensional modeling of a diesel engine can involve any given process or part of the engine, as modeling has become an intricate part of the design process. Computational models have been used to describe the flow properties in the cooling passages, handling such phenomena as boiling heat transfer [51], as well as computing the transport of heat from the cylinder gases to the cooling media of the water jacket, via conjugate heat transfer [52–54]. In many cases the need for simplification of the computational domain calls for the coupling of different tools. In many CFD studies, one-dimensional gas-exchange codes are used to provide initial values and/or boundary conditions for the simulations. In these cases, values from the one-dimensional tools are used to initiate the CFD simulations and even provide some boundary conditions to the simulations, as shown in [55].

CHAPTER 3

CFD Model

In order to evaluate the amount of heat transferred from the cylinder during a combustion process, all physical processes must be realistically represented. For that reason, the task in the CFD modeling of a CI engine is to solve the governing equations for unsteady, compressible, turbulent reacting flow with the introduction of fuel droplets. This requires a number of sub-models that each represents its own physical process.

3.1 Turbulence modeling

Having an accurate representation of the near-wall fluid flow is essential for a good heat transfer estimation. Not only does the near-wall flow field influence the amount of heat transferred from the cylinder, but also the bulk flow of the gas. There are three main conservation laws for the system of reactive, turbulent flows; conservation of mass, momentum and energy. From these laws, the necessary transport equations can be derived [56, 57]. Based on the law of mass conservation, the transport equation for mass is given by the continuity equation, shown in Eq. (3.1). The transport equation for momentum, based on the conservation of momentum, is shown in Eq. (3.2). This set of partial differential equations is usually referred to as the *Navier-Stokes equations*. The

transport equation for energy in the domain is given by the energy equation, shown in Eq. (3.3).

$$\frac{\partial \rho}{\partial t} + \frac{\partial \rho u_j}{\partial x_j} = 0 \tag{3.1}$$

$$\frac{\partial (\rho u_i)}{\partial t} + \frac{\partial (\rho u_i u_j)}{\partial x_j} = -\frac{\partial p \delta_{ij}}{\partial x_j} + \frac{\partial \tau_{ij}}{\partial x_j} \tag{3.2}$$

$$\frac{\partial \rho e_0}{\partial t} + \frac{\partial \rho u_j e_0}{\partial x_j} = -\frac{\partial u_j p}{\partial x_j} + \frac{\partial u_i \tau_{ij}}{\partial x_j} - \frac{\partial q_j}{\partial x_j} \tag{3.3}$$

The viscous stress, from Eqs. (3.2) and (3.3), is given by Eq. (3.4).

$$\tau_{ij} = \mu\Big(\frac{\partial u_i}{\partial x_j} + \frac{\partial u_j}{\partial x_i}\Big) - \frac{1}{3}\frac{\partial u_k}{\partial x_k}\delta_{ij} \tag{3.4}$$

Due to the non-linearity of the equation system described above, as well as the large spectra of turbulent eddies in an engine system, the direct analytic solution of the described equation system is difficult. In order to solve this analytically, the resolution in both time and space would have to be extremely fine, which would be difficult for even the most powerful modern computers to handle within a reasonable time limit. Therefore, the need for modeling has risen. There are three main families of turbulence modeling, *Direct Numerical Simulations* (DNS), *Large Eddy Simulations* (LES) and *Reynolds-Averaged Navier-Stokes* (RANS) models. These approaches differ in which part of the energy spectrum of the turbulent flow is solved and which are modeled.

In the DNS approach, the entire set of flow motion equations is solved directly on all scales. This approach requires an extremely fine resolution in both time and space and is therefore too computationally demanding to carry out for turbulent reacting flows in an engine system. This approach has been considered a feasible approach in low-to-moderate Reynolds number flows in small computational domains [56].

In LES, the large scale turbulence is resolved in the computational domain, while only the small scale turbulence is modeled. By this, the instantaneous fluctuations in the large scale turbulent motion are preserved, giving a realistic and accurate representation of the medium-to-large scale flow motion. With increasing computational power, this approach has become more appealing for engine simulations, though it has primarily been used for flow simulations. In the academic community, LES is increasingly being used for researching turbulent, reactive flows, for applications where instantaneous fluctuations are important.

3.1.1 RANS models

The Reynolds Averaged Navier-Stokes equations are the basis of the so-called RANS model group. In this approach, the entire turbulent energy spectrum is modeled, applying a Reynolds decomposition on the governing differential equations. This averaging process causes the RANS models to lose information on the fluctuations of the turbulent flow structures, as the model solution provides averaged values of the flow in each computational cell. When comparing data from simulations to experimental data, this can be an advantage because most, if not all, experimental data is presented as an average of multiple cycles. This can allow for a more direct comparison of mean values from simulation and experiments. Another advantage of the RANS models, is the relatively short computational time, compared to LES and DNS, which can allow for a numerical parameter variation within reasonable time limits. Because RANS is less computationally demanding than the other model groups, it has traditionally been used by engine developers to aid their design in the simulation process.

There are two main groups of RANS models; models with an *eddy viscosity based closure* and models with a *Reynolds stress closure* [56]. These groups are then further divided into sub-groups. The Reynolds stress models (RSM) have been shown to provide better results than the eddy viscosity models (EVM). However, the difference in computational time and memory requirement have resulted in the domination of EVM over RSM in the automotive community. The most widely used EVM's are different versions of the k-ϵ or the k-ω models, which are 2-equation EVM's. In these models, transport equations for the turbulent kinetic energy (k) and either the dissipation rate (ϵ) or specific dissipation rate (ω) are solved. These models are known to have difficulties to predict the flow motion correctly in certain conditions present in engine rotational flows. In some cases, modifications have been made to these models to improve the prediction for such cases, but then usually the computational time is increased [58].

An alternative to the standard two equation models is to use non-linear EVM's. The non-linear EVM's include a rotational tensor that improves the handling of rotational- and secondary flows. The model used for the work presented in this thesis is a non-linear EVM, $k-\zeta-f$, proposed by Hanjalic *et al.* [59]. It is based on the elliptic relaxation concept used in Durbin's v^2-f model [60], but introduces a velocity scale ratio, $\zeta=\overline{v^2}/k$, instead of solving the equation for the velocity v^2. This simplifies the near wall behavior and improves numerical stability. Popovac & Hanjalic even proposed a compound wall treatment [61, 62], which has been found to give improved results in applications with complex geometries, such as IC engine applications.

3.2 Combustion & emission modeling

Modeling of turbulent combustion in diesel engines is a challenging subject when coupled with RANS based turbulence modeling, because the turbulence model provides mean quantities in the computational cell. This provides a problem to the closure of the chemical source term, since the usage of mean quantities may cause deviation in ignition, combustion and emissions for simulations compared to experiments [63]. There are a number of options available for combustion modeling in CFD simulations and in the following sections, the models used for combustion and emission modeling in this theses are discussed.

3.2.1 Turbulence controlled combustion

Magnussen and Hjertager [64], proposed a combustion model based on the eddy break-up (EBU) concept. The model is based on the assumption that the mean turbulent reaction rate of combustion is determined by the rate of dissipation of the turbulent eddies, containing fuel and oxygen. The mean reaction rate of the fuel is given by Eq. (3.5).

$$\overline{\rho \dot{r}_{fu}} = \frac{C_{fu}}{\tau_R} \overline{\rho} \min\left(\overline{y}_{fu}, \frac{\overline{y}_{Ox}}{S}, \frac{C_{Pr}\,\overline{y}_{Pr}}{1+S}\right) \tag{3.5}$$

This model has previously been used in commercial CFD tools to predict diesel combustion and usually gives reasonable results. The main problem with the model is that it contains a number of model constants for the reaction rates, so it has to be calibrated for optimum use. This model required the use of a separate model for the auto-ignition process, where the shell auto-ignition model is usually preferred. The shell auto-ignition model was originally developed for knock prediction in gasoline engines [65], but has since been extended for diesel auto-ignition. The extension of the original model includes an improvement of the prediction with fuels of higher molecular weight, such as diesel fuel [66]. For a part of the work, presented in Paper II, the combination of these models has been used for conventional diesel combustion.

3.2.2 ECFM-3Z

The best known model utilizing homogeneous tabulation of auto-ignition chemistry is the ECFM-3Z model by Colin & Benkenida [67]. The acronym stands for the 3-zone extended coherent flame model, and the model was first presented in 2004. This is an extension of the previously existing extended coherent flame model, which was developed for SI engine combustion. The addition to the ECFM model, is that a mixing model has been added to be able to handle both single

and multiple fuel injections. Each computational cell is divided into three mixing zones, both for burnt gases and unburnt gases, resulting in a total of 6 zones in each computational cell, as shown in Fig. 3.1. The model was used for diesel

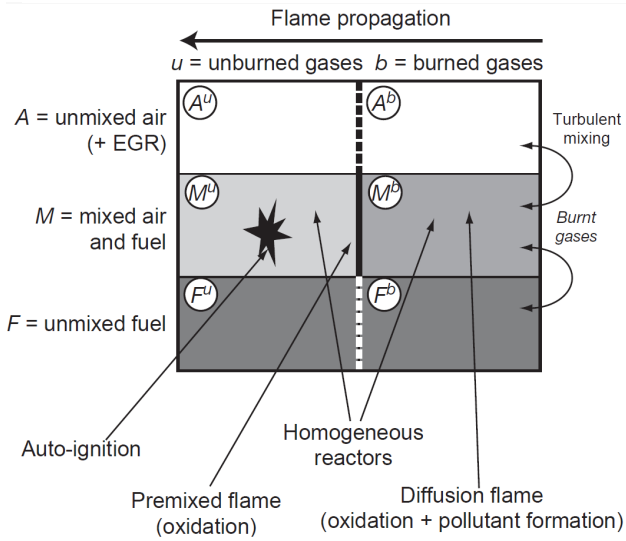

Figure 3.1: *Schematic of a computational cell in the ECFM-3Z model [67].*

combustion prediction in Paper I, and its capability to predict both premixed and diffusion flames was the premise for its selection to model PPC cases in Papers II and III. The model used in the papers is a further development of the original ECFM-3z, where the parametrization of the ignition process has been improved along with adding consideration of fluctuations of the mixture fraction on the diffusion flame equilibrium chemistry and the auto-ignition process. The consideration on the temperature fluctuations on the auto-ignition process has also been added, as discussed in [63].

3.2.3 Chemical kinetics of N-heptane

Although, the use of relatively simple combustion models can provide necessary information on the combustion process for a given fuel, it usually does not include detailed information on the intermediate species formed during combustion. These species can have a considerable effect on the auto-ignition process, as well as the equilibrium state of the combustion [68]. The composition of a commercial diesel fuel is extremely complex and highly variable, as stated by

Farrel *et al.* [69]. The presence of aromatics and cyclo-paraffins, in various quantities depending on the fuel origin, provides a challenging task of choosing an appropriate surrogate for the diesel fuel. The amount of aromatics in a diesel fuel can range from around 3% (Swedish MK1 diesel) to around 30% (US or EU diesel fuels) [69, 70]. N-heptane has become a popular surrogate fuel for diesel, because of its similar ignition qualities. However, due to high concentrations of aromatics and cyclo-paraffins, the reproduction of the pollutant formation process of a real diesel fuel with n-heptane chemistry is limited [69]. Additionally, the density and viscosity between n-heptane and diesel fuels differ, which will lead to different breakup and evaporation qualities between the fuels. Other surrogate fuels have been used for diesel combustion, including n-decane, which has both been used as a single component fuel or mixed with an aromatic species, such as toluene. Detailed kinetics of higher paraffins, containing two or more carbon atoms, are too complex to handle in multi-dimensional engine simulations, so a considerable effort has been put into reducing chemical schemes for simulation purposes. The largest effort has been put into reduced schemes for n-heptane, which has led to a variety of reaction mechanisms available for the use of n-heptane in diesel engines. These mechanisms differ considerably in their complexity. A full, detailed chemical mechanism for n-heptane is available from the Lawrence Livermore National Laboratory, where over 5000 reactions are considered [71–73]. Other authors have reduced the reaction mechanisms to produce alternatives that are more feasible for engine simulations. Tsurushima [74] published a PRF reaction mechanism consisting of 33 species and 38 reactions, while as a n-heptane or iso-octane mechanism, the number of species and reactions reduced to 24 and 25, respectively. The reaction mechanism used for Paper V is from the Engine Research Center in Wisconsin, Madison, US [75] where a mechanism containing 29 species and 52 reactions has been developed to simulate diesel fuel chemistry with n-heptane as a surrogate fuel. The mechanism was initially developed for HCCI combustion, but has also been used for diesel combustion, with good results.

One of the main reasons for the increased use of chemical kinetic schemes for combustion prediction in CFD simulations is the introduction of a multi-zone approach to the chemical kinetics solver. In the multi-zone approach, computational cells containing similar thermodynamic conditions, temperature and air-fuel ratio, are clustered and the chemical reactions are solved for the mean of each cluster of cells. After the chemical reactions have been evaluated for each cluster, the conditions are mapped back to each computational cell in the physical domain. This process is described in detail in [76] and has been incorporated in the study, presented in Paper V.

3.2.4 NO_x emissions

Oxides of nitrogen, nitric oxide (NO) and nitrogen dioxide (NO_2) are collectively know as NO_x in the combustion engine community. Generally, nitric oxide, or NO_x, formation stems from three main sources, which are named *thermal* NO_x, *prompt* NO_x and *fuel* NO_x. The principle source of NO is the oxidation of atmospheric nitrogen [3], therefore, NO_x formation from prompt and fuel NO_x are often neglected in engine simulations. For this reason, only thermal NO_x has been modeled in this work. The reaction mechanism for thermal NO_x is usually expressed in terms of the *extended Zeldovich mechanism*, given by Eqs. (3.6) to (3.8).

$$N_2 + O \underset{k_{1b}}{\overset{k_{1f}}{\longleftrightarrow}} NO + N \tag{3.6}$$

$$N + O_2 \underset{k_{2b}}{\overset{k_{2f}}{\longleftrightarrow}} NO + O \tag{3.7}$$

$$N + OH \underset{k_{3b}}{\overset{k_{3f}}{\longleftrightarrow}} NO + H \tag{3.8}$$

In Eqs. (3.6) to (3.8), the reaction rate constant k_{if} refers to the rate of the forward directed reaction i. At the same time the reaction rate constant k_{ib} refers to the rate of the backwards directed reaction i.

The model used in this work is based on the partial equilibrium assumption of the first two reactions of the extended Zeldovich mechanism. This leads to a global reaction approach for the thermal nitric oxide formation, according to Eq. (3.9).

$$N_2 + O_2 \longrightarrow 2NO \tag{3.9}$$

With the reaction rate constant, $k_f = k_{1f} \cdot k_{2f}$, the source term in the conservation equation for NO is given by Eq. (3.10).

$$\frac{\partial c_{NO}}{dt} = 2 k_f \, c_{N_2} c_{O_2} \tag{3.10}$$

3.2.5 Soot emissions

From the $\Phi - T$ map in Fig. 2.2, one can see that soot formation is present at fuel-rich conditions, at mid-to-high combustion temperatures. At these conditions, there is not enough oxygen in the cylinder gas-mixture to complete the soot-oxidation process, so the engine-out soot will be high. To include soot in the computation, an extra partial differential transport equation, for the mass fraction of soot, is added to the set of governing equations. The conservation of the soot mass fraction ϕ_s is shown in Eq. (3.11).

$$\frac{\partial}{\partial t}\left(\overline{\rho}\tilde{\phi}_s\right) + \frac{\partial}{\partial x_j}\left(\overline{\rho}\widetilde{u_j \phi_s}\right) = \frac{\partial}{\partial x_j}\left(\frac{\mu_{eff}}{\sigma_s}\frac{\partial \tilde{\phi}_s}{\partial x_j}\right) + S_{\phi_s} \tag{3.11}$$

The source term in Eq. (3.11), the soot formation rate, is given by

$$S_{\phi_s} = S_n + S_g + S_{O_2} \tag{3.12}$$

where the source is divided into sources from nucleation (n), surface growth (g) and oxidation (O_2).

A variety of models have been developed to represent the formation and oxidation of soot for CFD simulations, varying in their complexity, as demonstrated by Xi and Zhong [77] and Tao *et al.* [78]. Two frequently used models are the *Lund flamelet model* and the *Frolov kinetic model*. The former option considers contributions for the source term of the soot volume fraction, i.e., surface growth, oxidation, particle inception and fragmentation [79]. These four contributions can all be adjusted to the specific problem, by a scaling factor, which results in four scaling factors for the model. This model has been applied to the study presented in Paper I.

The latter option considers soot formation and oxidation based on a detailed chemical reaction scheme, where multiple mechanisms have been combined [80–86]. The complete detailed kinetics scheme of the soot formation process has been reduced for the applied soot model to a limited number of species and reactions. By this reduction the computational efficiency of the model is increased. In the CFD code, reactions constants have been incorporated for a few fuel types, including n-heptane. For fuel types differing from the available fuels in the solver, the most appropriate model constants are automatically decided. This implies that no ”tuning” is required by the user. This soot model has been applied to the studies presented in all papers, except Paper I.

3.3 Spray behavior

Liquid fuel sprays belong to a specific type of two-phase flows, characterized by a dominating direction of motion [87]. The liquid phase, which consists of droplets, is introduced into a gaseous volume where the droplets break up into smaller parcels and eventually evaporate. There are two major approaches used to describe the motion of liquid droplets, Eulerian and Lagrangian. The difference lies in how the characteristics of a single particle is handled, where in the Eulerian description, it is assumed that the characteristics can be described as a continuum, making use of the same discretization and similar numerical techniques as the continuum-phase. In the Lagrangian approach, the particle is described as a single point which moves with its own velocity [88]. The computational requirements are larger in the Eulerian approach, which has made the Lagrangian approach more dominant in liquid fuel spray modeling. In this work, the introduction of liquid droplets is modeled by using a statistical model, re-

ferred to as Discrete Droplet Method (DDM) [89], which is a Lagrangian particle tracking method.

Once the droplets are introduced into the computational volume, a breakup model must be applied to represent the breakup of large droplets into smaller ones, before they evaporate. There is a variety of breakup models available, but the two most frequently used models in RANS based CFD are the KH-RT model and the Wave breakup model. For the purpose of this thesis work, the Wave child breakup model has been applied. It is based on the standard Wave breakup model, introduced by Reitz [90], with the additional introduction of child droplet parcels in order to increase fuel vapor in the injector nozzle region. In the model, Reitz's blob injection strategy is used, meaning that the largest droplet has the same size as the injection hole diameter. In the model, there are six model constants (C_1-C_6), two of which are fixed (C_1 and C_3). One parameter (C_2) is used to estimate the characteristic breakup time, while parameters C_4 and C_5 control the size and number of child parcels. The distribution between the minimum stable diameter and the parent drop diameter is decided by the model parameter C_6.

To account for droplet evaporation the *heat and mass transfer analogy*, or the *Dukowicz* model, has been applied. This model is based upon the assumption of spherical symmetry, as well as assuming a quasi steady gas-film around the droplet. The droplets are assumed to be at a uniform temperature and uniform physical properties of the surrounding fluid are also assumed. There is an additional assumption of a liquid - vapor thermal equilibrium on the droplet surface, as presented by Dukowicz [6]. Even though this is a quite simple model for evaporation of liquid droplets in diesel sprays, it has been extensively used in CFD simulations, with decent results. However, if a detailed, accurate description of droplet evaporation is required, considerations must be made for the effect of thermal radiation and a finite thermal conductivity within the droplets, as pointed out by Sazhin *et al.* [7].

3.4 Wall heat transfer

The temperature of the fluid is obtained by solving the transport equation for enthalpy in each computational cell, which is derived from the energy equation, Eq. (3.3), rewritten in terms of enthalpy as shown in Eq. (3.13).

$$\rho\frac{DH}{Dt} = \rho\left(\frac{\partial H}{\partial t} + U_j\frac{\partial H}{\partial x_j}\right) = \rho\dot{q}_g + \frac{\partial P}{\partial t} + \frac{\partial}{\partial x_i}(U_j\tau_{ij}) + \frac{\partial}{\partial x_j}\left(\lambda\frac{\partial T}{\partial x_j}\right) \tag{3.13}$$

In the equation, the second term on the right hand side is a pressure-time derivative accounting for the contribution of local pressure rise to the energy

equation. The third term on the right hand side includes the contribution from viscous heating to the energy equation, while the source term, $\dot{q}_g$, contains all remaining sources to the energy equation, such as chemically released heat from combustion and radiation. All of these are included in the simulations, except for the effects of radiation in the source term, due to reasons stated in Section 2.3.3.

The turbulence model used is a high Reynolds number model, which requires special treatment of the near-wall region, to represent the boundary layer. This means that the heat transfer to the walls is estimated by a set of wall functions. There are three widely used wall function formulations available, as well as various modifications of those. The remainder of this section will describe the differences in the available wall functions.

3.4.1 The standard temperature wall function

A widely used and presented temperature wall function is the one introduced by Launder & Spalding in 1974 [91] as the best practice of the Imperial College of London, at that time. In some publications, this formulation has been referred to as the ”standard” or even ”simple” temperature wall function. It's basis is that the first computational point is sufficiently remote from the wall so that the viscous effects are overwhelmed by the inertial ones.

$$T^+ = \frac{\rho c_p u_\tau (T - T_w)}{q_w} = \sigma_T \left[u^+ + P\left(\frac{\mathrm{Pr}}{\sigma_T}\right)\right] \tag{3.14}$$

In the above equation, P is a correction function dependent on the ratio of laminar to turbulent Prandtl numbers, called the ”pee-function”. This model is by some considered to considerably under-predict wall heat transfer in engine simulations, since it neglects the variation of gas density in the boundary layer [49].

3.4.2 Angelberger wall function

One of the improvements to the temperature wall function formulation is the model presented by Angelberger *et al.* [92]. In this model, the variation of boundary layer gas density is taken into account and therefore it can be said that this is a compressible form of the ”standard” wall functions presented before. The formulation is given by Eq. (3.15).

$$T^+ = \frac{\rho u_\tau c_p T}{q_w} \ln\left(\frac{T_w}{T}\right) = \sigma_T \left[u^+ + P\left(\frac{\mathrm{Pr}}{\sigma_T}\right)\right] \tag{3.15}$$

3.4.3 Han & Reitz temperature wall function

In 1996, Han & Reitz proposed a wall temperature wall function for variable-density, turbulent flows in engines [93]. The formulation is based upon a few assumptions. The first assumption states that wall normal gradients are assumed to be much greater than tangential ones. The second assumption is that near-wall fluid velocity is directed parallel to the wall. The third assumption states that pressure gradients are neglected. The fourth assumption declares that viscous dissipation is neglected. The fifth assumption is that radiation heat transfer is neglected and finally the gas is considered to be ideal. Basing the derivation of the temperature profile on the one-dimensional formulation of the energy equation, the resulting profile is given by Eq. (3.16).

$$T^+ = 2.1\ln(y^+) + 2.1G^+y^+ + 33.4G^+ + 2.5 \tag{3.16}$$

where G^+ is a dimensionless source term in the energy equation, given by Eq. (3.17).

$$G^+ = \frac{G\nu}{q_w u^*}, \qquad G = \bar{Q}_c \tag{3.17}$$

where $\overline{Q}_c$ is the average chemical heat release. The corresponding wall flux formulation is given by Eq. (3.18).

$$q_w = \frac{\rho c_p u^+ T \ln(T/T_w) - (2.1y^+ + 33.4)G\nu/u^+}{2.1\ln(y^+) + 2.5} \tag{3.18}$$

If the source term G can be neglected, Eq. (3.18) will reduce to the rearranged form of Eq. (3.19).

$$T^+ = 2.1\ln(y^+) + 2.5 = \frac{\rho u_\tau c_p T}{q_w}\ln\left(\frac{T_w}{T}\right) \tag{3.19}$$

3.4.4 Other formulations of wall functions

Nuutinen *et al.* [50, 94] examined the formulation proposed by Han & Reitz and found that their formulation neglects the fact that the friction velocity u_τ should be a function of a variable density. Han & Reitz, however, had fixed their friction velocity to a certain density and then treated the density as a variable, treating the friction velocity as a constant. Nuutinen *et al.* then suggested an alternative choice of dimensionless parameters, keeping the remaining Han & Reitz formulation.

Rakopoulos *et al.* presented an overview of the most widely used wall functions for the energy equation and proceeded to present their own. Their analysis was based on the same principle as the Han & Reitz formulation and that of

Nuutinen *et al.*, namely the one-dimensional energy equation across the boundary layer, along with the continuity equation within the boundary layer [49]. Their analysis was performed for a motoring case, so the energy source from combustion was neglected. They however, included a pressure work term, which was neglected in the previously presented formulations. The resulting temperature profile is provided in Eq. (3.20) and the non-dimensional temperature term is given by Eq. (3.21).

$$\begin{aligned} T^+ = & \frac{1}{0.4767}\left[\ln\left(y^+ + \frac{1}{\mathrm{Pr}0.4767}\right) - \ln\left(40 + \frac{1}{\mathrm{Pr}0.4767}\right)\right] \\ & + 10.2384 + P^+\left(\frac{y^+ - 40 + 117.31(0.4767 + \frac{1}{\mathrm{Pr}}}{0.4767 + \frac{1}{\mathrm{Pr}}}\right) \end{aligned} \tag{3.20}$$

$$T^+ = \frac{\rho u_\tau c_p T}{q_w} \ln\left(\frac{T_w}{T}\right) \tag{3.21}$$

where P^+ is the non-dimensional pressure term, given in Eq. (3.22).

$$P^+ = \frac{\left(\frac{dP}{dt}\right)\upsilon}{q_w u_\tau} \tag{3.22}$$

CHAPTER 4

Modeled engines

Four diesel combustion engines have been modeled in this thesis work. Two of the engines are heavy-duty truck engines, where the engine geometry has been provided by the truck manufacturer Scania, in Södertälje. These engines are the 12 liter D12 engine and their Euro 5 compliant 13 liter D13 engine. The third engine is a light-duty car engine, provided by the Volvo Car Corporation, in Gothenburg, of their new Euro 6 compliant 4 cylinder architecture. The last engine is a medium-duty engine, which is based on a 4 cylinder, 4 liter AVL research engine. In all cases, only the in-cylinder process during the closed volume part of the cycle is considered, i.e., compression, combustion and expansion. Therefore, the engine is simulated from the time of inlet valve closing (IVC) to the time of exhaust valve opening (EVO). The computational domain encloses one of the fuel sprays, from the injector, applying periodic boundary conditions to the side wall boundaries. This means that for a engine with an injector nozzle with eight holes, only one-eighth of the cylinder volume is modeled. This implies considerable savings in computational time for a given engine simulation. An example of a computational domain is provided in Fig. 4.1. In such a model, there are three wall boundaries; the cylinder head- and liner boundaries as well as the piston wall boundary. There is also an extra volume in the crevice area, which is scaled to provide the accurate compression ratio. This volume is usually considered to have adiabatic properties.

4.1 Scania D12 truck engine

The 12 liter Scania truck engine, D12, was used in Paper IV to study the effects of fuel quality and injection strategy on a heavy duty PPC engine. The specifications of a single cylinder of the engine, as well as the computational domain, are shown in Fig. 4.1. The valve timings for IVC and EVO are provided because they signal the start and end timings of the simulation, respectively. The geometrical compression ratio of 18:1 was adjusted in the calculations to provide a better match of the mean cylinder pressure, provided from the experimental data. The number of orifices in the injector nozzle was the defining factor for the size of the computational domain, since only one of the fuel sprays has been modeled in the closed volume simulation. The introduction of fuel parcels in the model is done by a blob-injection, where the largest droplets are the same size as the injector orifice hole. This means that the largest droplets in the domain for the D12 engine were 0.18 mm in diameter. The experimental data used for validation of the models for this engine were published by Manente *et al.* [95], where the engine, modified for single cylinder operation, was run in PPC mode with nine different gasoline fuels. The idea in [95] was to investigate what effects fuel quality has on the combustion concept, ranging the octane number of the nine fuels from 69.4 to 99 (RON). The results were quite promising, as all cases demonstrated a gross indicated efficiency above 50%, along with low emission levels. In Paper IV, two of the nine gasoline fuels in the study were simulated and compared, along with two different injection strategies. The difference in heat transfer and engine performance for the simulated cases was studied.

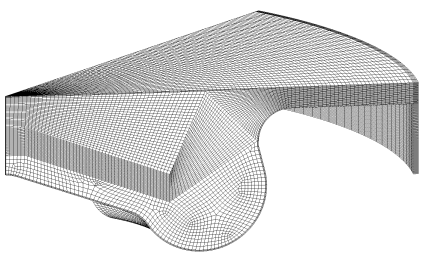

Displacement [cc]	1966
Bore x Stroke [mm]	127.5 x 154.0
Comp. Ratio [-]	18.0
Inlet valve closing	29 ° ABDC
Exhaust valve open	34 ° BBDC
Orifices [-]	8

Figure 4.1: *Left: Scania D12 engine segment, from Paper IV, at TDC. Right: Engine specifications.*

4.2 Scania D13 truck engine

The Scania D13 engine was used for the simulation work in Paper II and III, both in diesel and PPC conditions. The engine specifications and the computational domain, at TDC, are shown in Fig. 4.2. The engine has a slightly lower compression ratio, compared to the D12 engine, and the spray angle and injector hole size have changed. The biggest difference between the engines is the change in bowl type, as can be seen from a comparison between Figs. 4.1 and 4.2. In Paper II, the engine was run under both PPC and diesel conditions comparing the two combustion modes when the wall boundary conditions changed from normal to adiabatic. The experimental cases, used for validation for the D13 engine had two sources. For diesel operation, the validation data was provided by the engine manufacturer, Scania, while the engine data for the PPC operation was published by Manente *et al.* [16]. In that study, the engine was modified for single cylinder operation and run on 11 different fuels, nine gasoline fuels, one diesel fuel (Swedish MK1) and a primary reference fuel (PRF20). In Paper III the PPC case from Paper II was used in order to estimate the effect of inlet conditions and wall temperatures on engine heat transfer and performance. A design of experiments with five factors was used to create a meta-model, which was used to optimize the selected parameters.

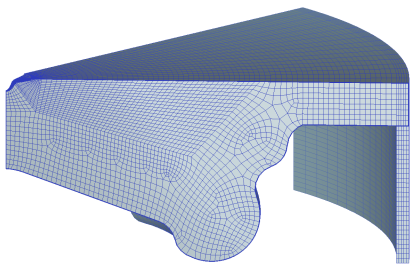

Displacement [cc]	2124
Bore x Stroke [mm]	130.0 x 160.0
Comp. Ratio [-]	17.3
Inlet valve closing	40 ° ABDC
Exhaust valve open	50 ° BBDC
Orifices [-]	8

Figure 4.2: *Left: Scania D13 engine segment, from Paper II & III, at TDC. Right: Engine specifications.*

4.3 Volvo light-duty engine

In Paper V, a light-duty engine from the Volvo Car Corporation was modeled to study the effects of the piston geometry and swirl levels on engine heat transfer. The computational domain, at TDC, as well as the engine specifications are shown in Fig. 4.3. The experimental data was provided by the manufacturer and contained single cylinder engine tests for three operating conditions for conventional diesel combustion. In the study, presented in Paper V, the engine sector model was validated for all three operating points, which were then used as baseline cases for a geometry and swirl level variation. By this variation, the effects of the piston bowl geometry in combination with different swirl levels on engine heat transfer were examined. For comparison, three alternative piston shapes were selected. The bore, stroke and combustion chamber volume for the three additional pistons were scaled to match the reference piston.

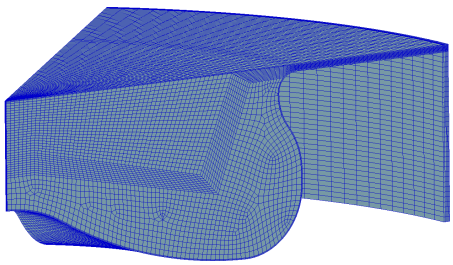

Displacement [cc]	492
Bore [mm]	82.0
Stroke [mm]	93.2
Comp. Ratio [-]	15.8

Figure 4.3: *Left: Volvo Euro VI engine segment, from Paper V, at TDC. Right: Engine specifications.*

4.4 AVL medium-duty research engine

This medium-duty engine from AVL was used for simulations in Paper I, using diesel fuel with conventional diesel combustion. The influence of 6 parameters on heat transfer and work output of the engine was examined. These parameters were; engine speed, egr, swirl, injection duration, spray angle and number of injection nozzles. The engine dimensions and shape, along with the operating- and boundary conditions, were provided by AVL. The specifications of the engine and the computational domain, at TDC, are shown in Fig. 4.4. The engine has 7 injector hole in the baseline configuration, leading to the simulation of one-seventh of the engine cylinder in the sector model.

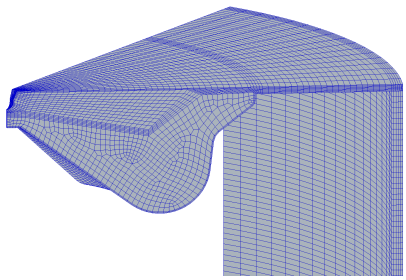

Displacement [cc]	1039
Bore x Stroke [mm]	105.0 x 120.0
Comp. Ratio [-]	16.0
Inlet valve close	20 ° ABDC
Exhaust valve open	50 ° BBDC
Orifices [-]	7

Figure 4.4: *Left: AVL engine segment, from Paper I, at TDC. Right: Engine specifications.*

CHAPTER 5

Results & discussion

5.1 Medium-duty engine heat transfer

The medium-duty AVL research engine was simulated using a baseline case with 7 injector holes and an injection angle of 160 degrees. Six parameters were varied around the baseline configuration, as demonstrated in Table 5.1. The table presents the baseline case in the middle column, with the low and high values on the left and right, respectively, resulting in three levels for each parameter.

Table 5.1: *Engine conditions for the AVL research engine [96]*

Parameter	Low value	Baseline value	High value
Engine speed [rpm]	2000	2500	3000
EGR [%]	25	28	35
Injection duration [deg]	30	32	34
Swirl [-]	1.4	1.5	1.8
Spray angle [deg]	140	160	180
Number of injector holes	6	7	8

The most interesting results from the variation, which is presented in Paper I, were obtained for the injection parameters, which gave the largest effect on the combustion. This resulted in altered cylinder temperatures and consequently

changed wall heat fluxes. It is important to bear in mind that some of the variations were, in hindsight, quite modest, as was the case for EGR, for instance. The EGR variations only consider an interval between 25% and 35%, around a reference that has the value of 28%. Comparing these values to the high EGR levels of PPC (around 50%), it is obvious that this is quite modest. Nonetheless, subtle differences in heat release rates for different EGR levels could be observed, as shown in Fig. 5.1. The figure shows heat released from combustion as a function of cranck-angle degree for the three modeled EGR levels. It shows that the diffusion part of the flame is slightly retarded for higher EGR levels, compared to the lower levels, which was to be expected due to the fact that EGR is an inert gas that, if introduced in large enough quantity, essentially lowers combustion temperature and can affect the ignition delay of the fuel. Larger variations in EGR would have provided a stronger difference in the heat release rate of the combustion. Examining the heat fluxes for the EGR variation, it revealed a small difference in the total heat flux of the engine. A lower EGR level increased the heat flux out through the engine walls, while the increase of EGR had the opposite effect. This was again due to the effects EGR has on combustion temperature, which leads to less exposure of the engine walls to higher gas temperatures.

Another interesting discovery from the study was the effects the injection properties had on combustion and heat transfer. A fundamental issue of directing the spray onto the optimal target became obvious when varying the spray angle from 140 degrees to the extreme of 180 degrees, which would be in-line with the cylinder head surface. As expected, the 180 degree spray angle provided poor results, with regards to combustion efficiency and work output. The change of spray angle from 140 to 160 had an effect on the the late, diffusion flame in

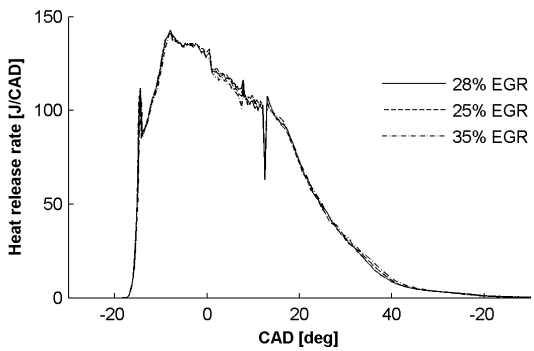

Figure 5.1: *Rate of heat release at varied EGR fractions [96].*

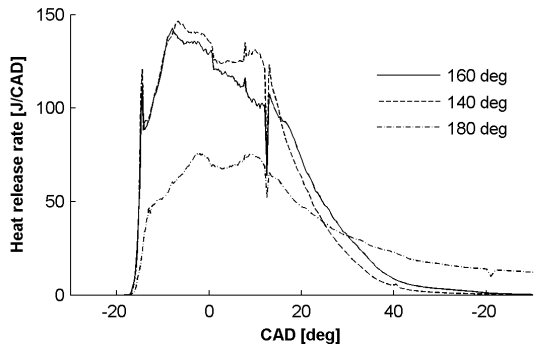

Figure 5.2: *Rate of heat release at varied injection angles [96].*

the combustion phase, where the narrow angle performed better, as shown in Fig. 5.2. This is due to the geometry of the combustion bowl and the mixing of fuel and air at the time of combustion. The work output was increased by 1.6% while the net heat transfer was reduced. This is because the combustion is moved further into the combustion bowl and away from both the cylinder head and liner surfaces, so the total heat transfer area, where high temperature gases are present, is reduced. This was supported by examining the average heat transfer coefficient, which was nearly unchanged for each of the surfaces in the model, so the bulk gas flow had not changed significantly.

A change in the injection duration changed the profile of the fuel flow in the cylinder, affecting the turbulent structures in the combustion bowl area. This caused a change in the heat transfer coefficient and consequently in the wall

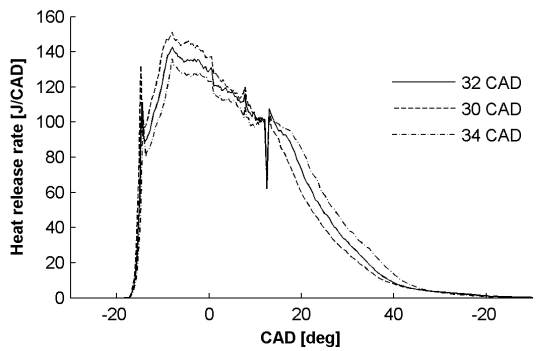

Figure 5.3: *Rate of heat release at varied injection durations [96].*

heat flux. This change in turbulent structures also had an effect on the rate of heat release from combustion, as shown in Fig. 5.3.

5.2 Adiabatic diesel and PPC engines

The heavy duty, Scania D13 truck engine was operated with both conventional diesel combustion and PPC modes. Both combustion cases were high load cases, with high pressure intake air, running at the same engine speed. The baseline cases, matched to experimental data, were used as basis for a low heat rejection study, comparing the results from diesel combustion to the PPC mode. Heat flux boundary conditions were applied, scaling from 100% (baseline), in 25% increments down to adiabatic conditions. The results showed that the trends in fuel consumption, efficiency and work output were in the line of what was to be expected for both engines, i.e., fuel consumption was reduced, while both efficiency and work output were increased with reduced heat losses, as shown in Fig. 5.4. Figure 5.4a shows the performance of the diesel mode, in terms of specific fuel consumption, gross indicated efficiency and indicated mean effective pressure (IMEP) for the closed volume part of the cycle (IVC-EVO). Figure 5.4b shows the same thing for the engine in PPC mode. Interestingly, the gross indicated efficiency gains, going from 25% heat load to adiabatic conditions, is relatively small, compared to the other increments. This small increase in efficiency is related to an increase in exhaust energy, where the last piece of heat loss reduction has not resulted in the same increase in work output, as in the other increments.

The response in emission production, however, was more surprising. Figure 5.5 shows the production of NO_x and soot, as well as the oxidation of soot as

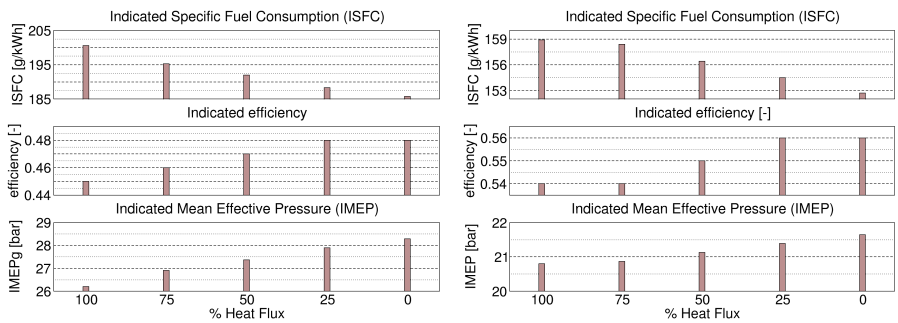

(a) *Diesel combustion* **(b)** *Partially premixed combustion*

Figure 5.4: *Engine performance with decreasing heat flux [19].*

a function of crank-angle degrees. Figure 5.5a shows the NO_x and soot emissions for the diesel combustion case, while the same emissions are shown in Fig. 5.5b for the PPC mode. It is important to note that the axis do not have the same scale, when making the comparison between the diesel and PPC modes. While the diesel combustion case showed a considerable increase in NOx emissions, the PPC case showed a less dramatic change. In both cases "engine out" soot emissions were relatively unaffected. The reason for the difference in NOx emission production between the cases can be traced back to the temperature during combustion, which is lower in the PPC case. Even though the global average temperature in both cases is below 1800K at the maximum, NOx emissions, which start to form at around 2200K, are formed in the diesel case but not as much in the PPC case.

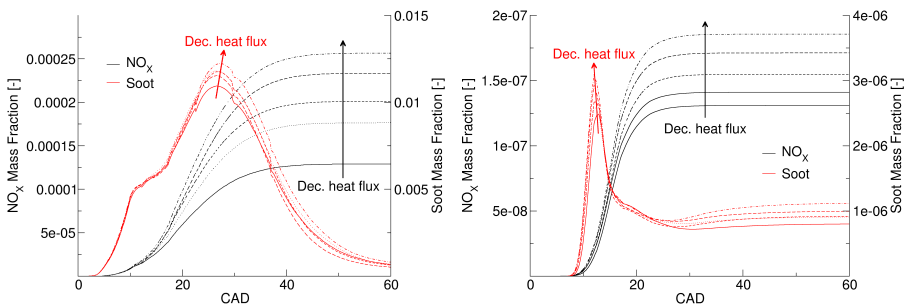

(a) *Diesel combustion* **(b)** *Partially premixed combustion*

Figure 5.5: *NOx and soot emissions with decreasing heat flux [19].*

A reason for this is found in Figs. 5.6 and 5.7, where the temperature distribution and equivalence ratio at 20 CAD after TDC are compared for the diesel and PPC cases, in a cut-plane through the center of the spray. The figures highlight the difference between the diesel and PPC modes. As the diesel case is more spray driven, higher amount of fuel is transported close to the piston wall, causing combustion to occur close to the wall. In the PPC case, the mixture is more premixed before combustion starts, which gives lower fuel concentration close to the walls and the combustion occurs further away from the wall. Looking at the temperature profiles in Fig. 5.6, it can be seen that the diesel case has high temperature combustion products flowing directly onto the piston wall surface and transporting towards the cylinder head and liner. At the same time, in the PPC case, temperatures during the combustion event stay below 1800-1900K, which is too low for the activation of NO_x formation, according to the $\Phi - T$ diagram presented in Chapter 1.

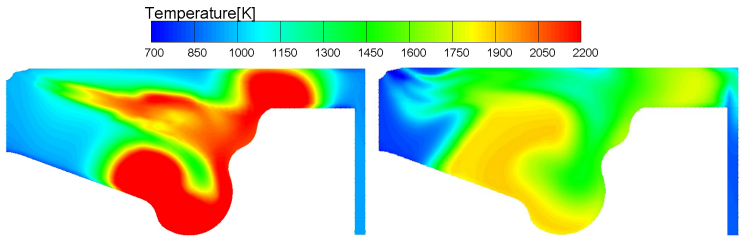

(a) *Diesel combustion* **(b)** *PPC mode*

Figure 5.6: *Temperature distribution at 20 CAD ATDC [19].*

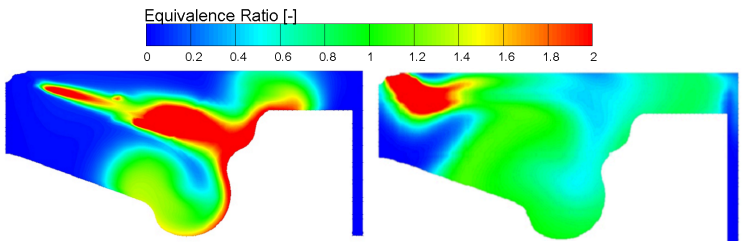

(a) *Diesel combustion* **(b)** *PPC mode*

Figure 5.7: *Equivalence ratio at 20 CAD ATDC [19].*

5.3 Optimization of IVC conditions

One way of affecting the combustion in the engine is by altering the inlet conditions of air. A study, where a meta model was used to optimize five parameters, within a decided parameter range, was presented in Paper III. This was done in the same Scania D13 engine as was used in Paper II, but only for partially premixed combustion mode. The meta model was constructed out of results from a simulation plan made using a design of experiments (DoE) methodology. The result matrix consisted of 5 parameters and four responses, which was the result of 27 simulation runs, to cover all combinations. The resulting meta-model was a second-order linear regression model, used to fit the five parameters to each of the four selected response variables which were; total, time averaged heat flux, IMEPg, NOx and soot emissions. A Genetic Algorithm (GA) was used to optimize the meta-model, yielding a solution to the five model parameters. These model parameters were the inlet pressure and temperature, along with all three wall boundary temperatures in the model.

Figure 5.8 shows a pressure-volume (pV) plot for the D13 engine operated in PPC mode with two different inlet air pressures. The engine was run at 75% load with high boosting pressure (3.66 bar) and low inlet temperature. EGR levels were also high (55%) and injection pressure was high (2400 bar). The figure shows that the work output was increased as inlet pressure was increased. However, this simulation did not include the gas exchange process, so the effects of the pumping loop is neglected. This is will have a significant effect when the boosting pressure is as high, as in this study.

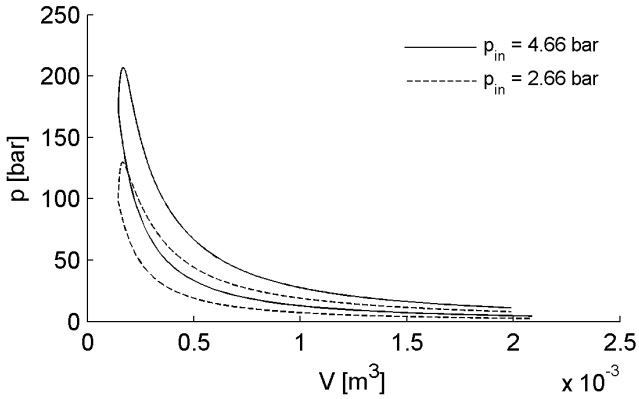

Figure 5.8: *pV plot with different inlet air pressures [20].*

The optimization of the meta-model showed that the best combination for reduced emissions and increased work output, with reduced heat losses, was a high boosting pressure, low inlet temperature and moderate wall temperatures. The fact that the inlet temperature should be low can be explained by Fig. 5.9, where a pV-plot is demonstrated for two cycles with different air intake temperatures. The decreased temperature will help to provide more favorable conditions at TDC, with higher peak pressure due to a more dense inlet air charge. This leads to a larger area in the pV-plot, which is equivalent to the work output of the engine.

The effect of inlet air temperature is also visible in Fig. 5.10, where heat released from combustion, as a function of crank-angle degrees, is shown for the two extreme inlet air temperatures. The figure shows that the cooler inlet air charge has a longer ignition delay than the hotter charge. However, the cooler charge has a more rapid combustion, which is favorable from a thermodynamic point of view. The ideal case would be to have an instantaneous, constant volume, heat addition, which would on the other hand cause too large pressure derivatives, causing engine noise or even malfunction. The conclusion for the engine

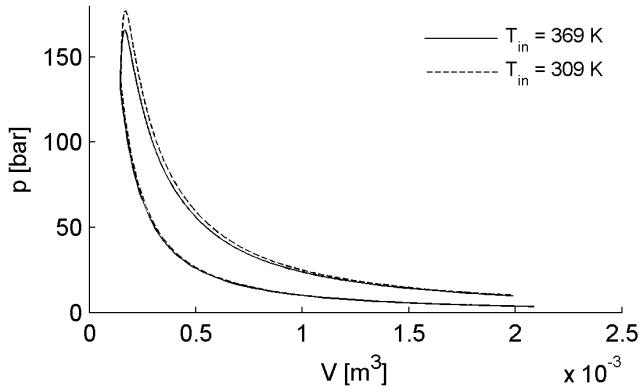

Figure 5.9: *pV plot with different inlet air temperatures [20].*

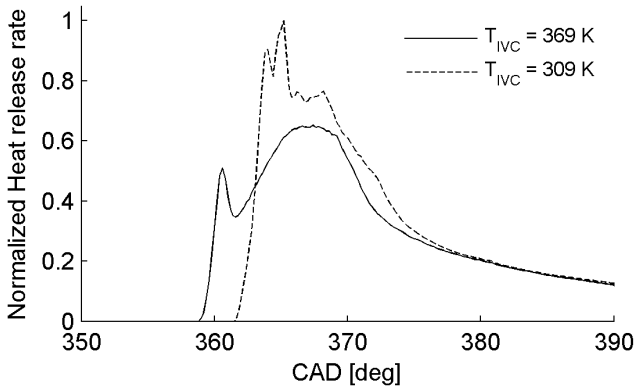

Figure 5.10: *Heat release rates for different inlet air temperatures [20].*

operating condition from this study was to aim for a cold pressurized charge in the inlet, mixed with enough EGR to control the combustion temperature and emissions.

5.4 Fuel quality and injection strategy

The Scania D12 engine was used in a study, presented in Paper IV, where two gasoline fuels were run in a compression ignition engine in PPC mode. The fuels were modeled with different combinations of three components that comprised the fuel; iso-octnae, n-heptane and toluene. Four cases were constructed, two for each fuel, where the engine load was altered for one of the fuels and the injection strategy for the other fuel. The change in injection strategy means that the simulations were run with a single injection, except for one load point which is run with a pilot injection at -60 CAD. Table 5.2 highlights the differences between the simulation cases in the study.

Table 5.2: *Simulated cases in [21]*

	Case 1	Case 2	Case 3	Case 4
RON	69	69	89	89
$IMEP_g$ [bar]	7.3	12.0	12.3	12.3
Pilot injection [CAD]	-	-	-60	-

The case that had the highest documented gross indicated efficiency in the experimental data, was the low load, single injection case. However, compared to the other cases, this case had the highest relative heat losses, which was mainly due to lower exhaust losses. The total fuel energy amount, available for thermodynamic conversion, was lower in this case, as it was a lower load case. This resulted in a lower exhaust energy, more efficient energy conversion of the released heat, but at the same time a higher fraction of the fuel energy as heat losses. Increasing the injected fuel mass, and increasing the engine load, generally did not yield an increase in the thermodynamic efficiency, but rather increased the exhaust gas energy. At the same time, it was shown that introducing a pilot injection resulted in a positive effect on the heat losses. This is believed to be due to better mixing of fuel and air, which provided a more thermally stratified charge. This lead to less exposure of hot gases to the engine walls, while the near-wall gases were colder than in the other cases. Figure 5.11 shows the direction of heat transfer for all four cases, i.e., where the piston surface is shown to experiences the largest amount of heat load. In the simulations, no significant effects on engine heat transfer could be established from the fuel quality alone. However, the presence of the early pilot injection was shown to have benefits with regards to heat transfer, as can be seen from the temperature distribution at 17 CAD ATDC in Fig. 5.12. Without the pilot injection, there was more fuel present in the near wall region, causing combustion to occur closer to the piston wall surface, consequently, giving rise to hotter gases in the near-wall region. These

results demonstrate the importance of the correct injection strategy for the best possible mixture of fuel and air in the engine cylinder, at the right location in the combustion bowl.

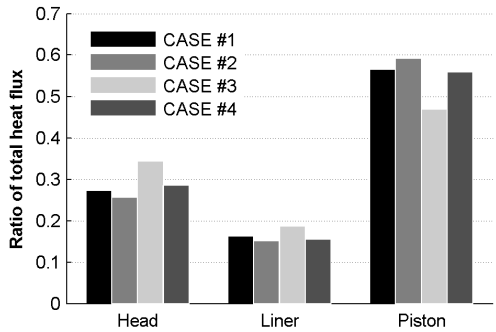

Figure 5.11: *Distribution of heat transfer [21].*

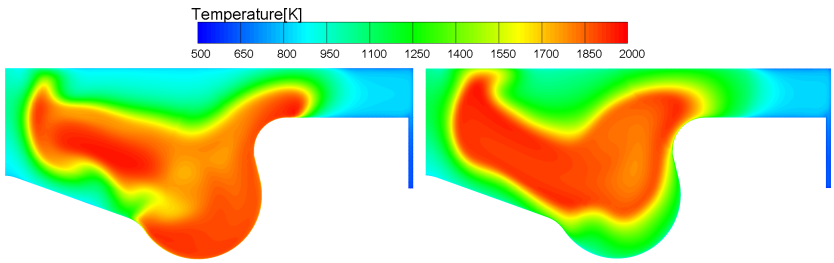

(a) *Single injection, low octane case.* **(b)** *Double inj., high octane case.*

Figure 5.12: *Comparison of pilot assisted and non-pilot assisted combustion. Temperature distribution at 17 CAD ATDC [21].*

5.5 Geometry effects

Making a change to the geometry of the combustion chamber is bound to affect the in-cylinder flow structures, as well as have influence on engine performance, emission levels and heat transfer. In the study presented in Paper V, a variation was made to the piston bowl surface, with the baseline of the new Euro 6, Volvo Cars combustion chamber. Three additional piston shapes were used in the study, while the volume of the combustion bowls, as well as the compression ratios were matched to the baseline case. Figure 5.13 shows the variation in geometry for the light-duty car engine, presented in Chapter 4. The three additional piston bowl shapes, which were all taken from available publications, were the older, Euro 5 Volvo Cars piston shape from Andersson *et al.* [97], a stepped, double re-entrant bowl from the Ford Motor Company [98] and a more open combustion chamber piston from the Toyota Motor Company [99]. All combustion bowls were modeled with the same configuration as the baseline bowl, aside from small variations in the spray angle, as explained in Paper V.

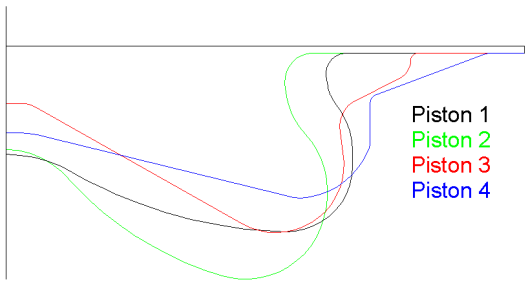

Figure 5.13: *Combustion chamber shapes with different piston bowl geometry [100].*

These combustion bowls were simulated at three load points with two swirl levels, resulting in 27 simulation runs. The normalized emissions of soot and NO_x are shown in Fig. 5.14, for all simulation cases. The results showed that the baseline bowl, Piston 1, had the most consistent emission performance, where emission levels were quite low for all loads. The double re-entrant bowl, Piston 3, also generated good emission levels, apart from one high-sooting point at low swirl conditions. The Volvo Euro 5 piston, Piston 2, and the Toyota piston, Piston 4, were in some sense outliers in the emission performance, as Piston 4 produced high amounts of NO_x, while Piston 2 produced high soot levels at some low-swirling conditions.

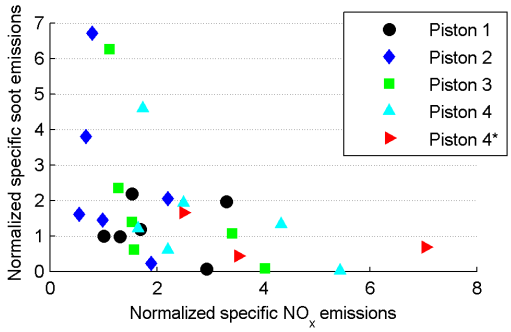

Figure 5.14: *Normalized specific soot-NO_x emissions. Filled symbols: high-swirl, non-filled symbols: low-swirl [100].*

In terms of heat transfer, Piston 3 was the best performing piston, as it demonstrated lower heat losses, than the other pistons, at all operating conditions. However, the piston that showed the best thermodynamic efficiency was, consistently, Piston 4. This indicates that even though a geometry demonstrates low heat losses, it does not directly translate into a high thermodynamic efficiency. Table 5.3 presents the normalized surface-to-volume ratio for all pistons in the study, along with information on the combustion phasing. CA50 indicates the crank-angle position where half of the fuel mass has been burnt, while CA90-10 indicates the duration, in crank-angle degrees, between 10% and 90% of the fuel mass is burnt.

Table 5.3: *Normalized surface-to-volume ratio and combustion duration for the pistons in [100]*

	Piston 1	Piston 2	Piston 3	Piston 4
Surface/volume	1.0	1.07	0.92	0.87
CA50 [CAD]	18.3	19.8	17.6	17.6
CA90-10 [CAD]	39.8	52.8	55.4	42.7

Intuitively, one would assume that having a low surface-to-volume ratio would provide low heat losses, as the contact area is reduced. This was not the case in this study, as the piston showing the lowest heat losses, was not the one with the lowest surface-to-volume ratio. Figure 5.15 demonstrates the total, time resolved heat flux for all pistons, for the full load case, at high swirling-conditions. In the early part of the heat flux curve, before combustion starts, the surface-to-volume ratio directly influences the heat transfer to the engine walls.

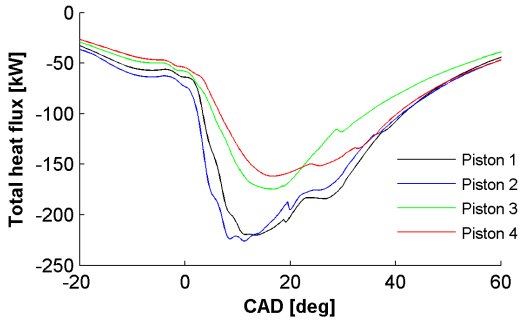

Figure 5.15: *Total, time resolved heat flux for the full load case at high swirl conditions [100].*

Figure 5.16 shows the heat released from combustion, normalized to the peak heat release from Piston 1. Comparing the heat flux and the heat release, it can be seen that after the start of the spray-driven combustion the heat transfer characteristics are changed. At this point, the combustion parameters and in-cylinder, spray-induced turbulence have more influence on the wall heat transfer than the surface-to-volume ratio. The comparison also shows that a shorter peak heat release, as is experienced by Piston 3, results in a shorter peak in heat flux.

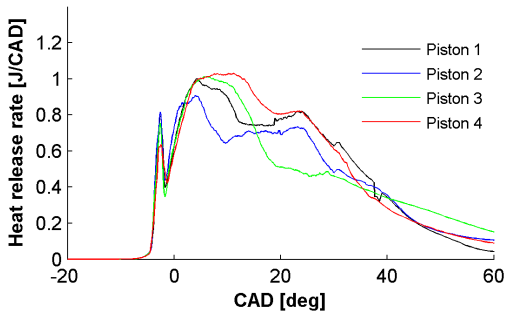

Figure 5.16: *Normalized heat release from combustion for the full load case at high swirl [100].*

This also gives rise to a lower in-cylinder gas temperature, as is shown in Fig. 5.17. The figure shows the average cylinder temperature for all pistons, for the full load case in the high-swirling configuration, where Piston 3 shows the

lowest in-cylinder temperature, along with Piston 2. This, along with the low surface-to-volume ratio, is the reason for the lowest heat flux for Piston 3. The reason for Piston 3 not being the most thermodynamically efficient geometry, is found in the combustion duration. Table 5.3 shows that the combustion duration (CA90-10) is shorter for Piston 4, than for Piston 3, which explains why the thermodynamic efficiency is higher for Piston 4. The exhaust temperature is higher for pistons 3 and 4, than for the other two pistons, as a result of the lower heat losses. The higher exhaust temperature can potentially be exploited for increased engine efficiency by extended expansion, reduced boosting work or with a waste heat recovery system

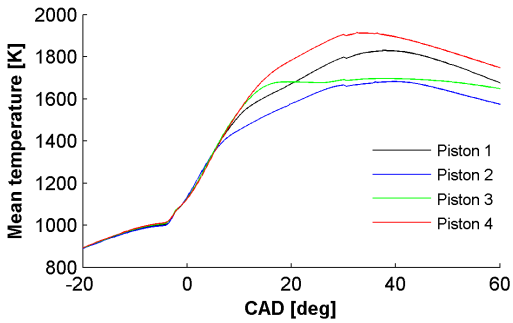

Figure 5.17: *Global averaged cylinder temperature for the full load case at high swirl [100].*

The effects of swirl were not consistent in the study, meaning that changing to a lower swirl number provided reduced heat transfer in pistons 1 and 2, but the opposite was experienced in Piston 4. Piston 3, however, experienced little or no variations in heat flux with reduced swirl. This can be traced back to the different effects of swirl on the in-cylinder fluid motion for each of the piston geometries, as shown in Fig. 5.18. The figure shows velocity profiles for all of the full load cases, both for high- and low swirl. It shows that the reduced swirl level reduces the velocities in the combustion bowl of the more conventional diesel combustion bowls, whereas limited or no such effect is visualized in the other two combustion bowls. This gives rise to the different response in heat flux for the reduction of swirl ratio in the individual piston bowls. However, reducing the swirl level further, to near-zero swirl, demonstrated positive effects. Using the configuration presented in the study Hashizume *et al.* [99], the statement from their publication could be confirmed. It stated that reducing the in-cylinder flow, by reducing swirling flow and limiting gas flow, by using a more open combustion chamber design, did in-fact reduce heat losses in the engine. This indicates that

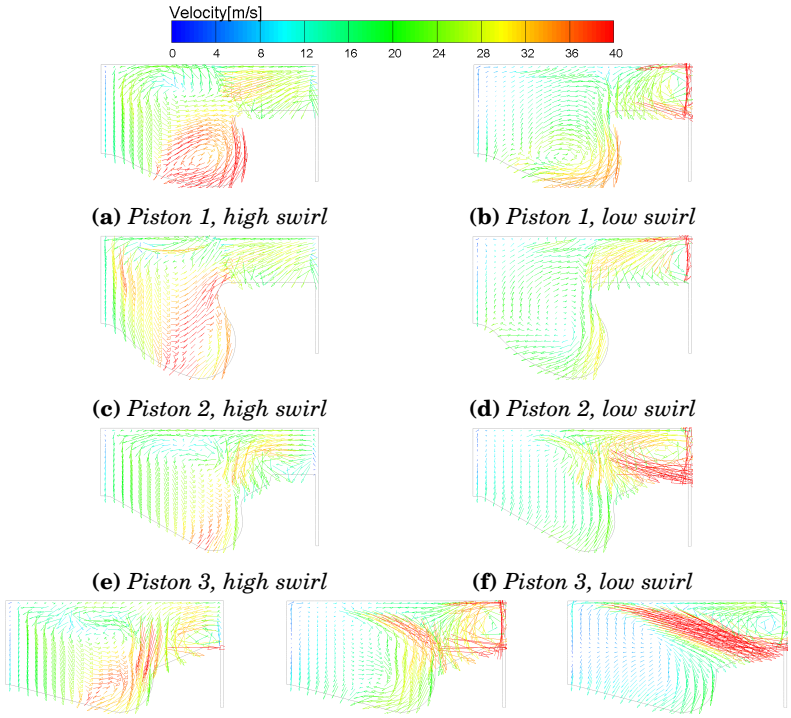

(a) *Piston 1, high swirl* **(b)** *Piston 1, low swirl*

(c) *Piston 2, high swirl* **(d)** *Piston 2, low swirl*

(e) *Piston 3, high swirl* **(f)** *Piston 3, low swirl*

(g) *Piston 4, high swirl* **(h)** *Piston 4, low swirl* **(i)** *Piston 4, no swirl*

Figure 5.18: *Velocity vectors in all combustion chambers at 30 CAD ATDC [100].*

the swirl level is equally as important as the geometry itself, when designing for reduced heat transfer.

5.6 Diesel vs. PPC engines

The work presented in this doctoral thesis has highlighted certain differences between diesel and partially premixed combustion modes. From Paper II the different reaction towards lower heat rejection on emission production and performance was shown. The results showed that a PPC engine operating at the same load output as a corresponding conventional diesel engine, emits a lower amount of NO_x emissions without showing an increase in soot emissions. When lowering combustion temperature in conventional diesel combustion with the

introduction of EGR in the intake, increased soot emissions have been observed, which was not the case in the PPC mode studied. In this context it can be stated that the requirements for the design of combustion bowl are different for diesel combustion, than for PPC. In order to obtain the optimal trade-off between NO_x and soot emissions, without compromising combustion efficiency, an efficient air-fuel mixture is beneficial. For PPC, these requirements are different, where the mixing process during the spray event is not as important, as the fuel is injected prior to the start of combustion. In the case of PPC, the air-fuel mixing prior to start of combustion is more important, which highlights the need for an optimal injection strategy, as pointed out in Paper IV, where the importance of a pilot injection was shown. Revisiting the results of Paper V, with the different requirements of diesel combustion and PPC in mind, it can be assumed that Piston 4 could be a good candidate for PPC studies, as it limits in-cylinder gas motion and shows reduction in heat transfer, compared to the conventional diesel piston bowls. Piston 3 resembles the piston shape of the Scania D13 engine, which has been used in heavy-duty PPC experiment and simulation work. The enhanced engine performance with the PPC mode has, partly, been credited to its low heat loss characteristics, as has been shown in this thesis. As for conventional diesel combustion, a piston in the style of piston 1 is quite efficient, both in terms of emission performance and heat transfer. However, in Paper V, the largest heat flux was shown to occur at the piston lip, which leads to the assumption that with slight modifications to the piston lip and squish flow, this piston might be further improved to experience simultaneous low emissions and low heat transfer.

CHAPTER 6

Conclusion and future outlook

The heat transfer process in diesel and PPC engines has been studied, using three-dimensional computational fluid dynamics simulations. The CFD models were used to recreate experimental results from single-cylinder engine tests for the investigation of temperature distribution and heat transfer in the engine cylinder. The engine model was used to perform simulations of varied engine parameters and geometrical parameters to investigate the response in heat transfer and engine performance, in order to provide information for improved engine design with minimized heat losses from the engine.

Varying a set of parameters in a medium-duty geometry, it was concluded that the largest effects on engine heat transfer came from variation in injection related parameters. There were some effects noticeable from EGR and swirl variations, but they were too modestly varied to show a large contribution.

The comparison of diesel and PPC engines, with regards to lower heat rejection engine operation, showed that a diesel engine has a larger relative heat loss than a PPC engine. Moving towards adiabatic conditions, both engines showed favorable performance values, showing an improvement in both work output and fuel consumption, while only the PPC engine could manage this without considerable increase in NO_x and soot emissions.

The PPC engine case was then used for investigation of the influence of inlet conditions and wall temperatures in the model, on heat transfer, engine performance and emission levels. From a meta-model derived from the results of a Design of Experiments matrix, it was shown that the combination of cold,

high pressure air, together with relatively high wall temperatures, provided the optimum solution, within the parameter space.

Investigating the effects of fuel quality and injection strategy on heat transfer in a PPC engine showed no real contribution of the fuel quality itself, while a favorable injection strategy could provide a thermal stratification of the in-cylinder gas. This stratification shielded the engine walls from the highest temperature gases, resulting in reduced wall heat transfer. However, this did not lead to an improved engine efficiency directly, but moved the energy loss towards the engine exhaust, through an increased exhaust enthalpy.

The geometrical effects on heat transfer in a light-duty passenger car engine were also investigated and found to be significant. Providing a geometry with an open combustion chamber, results in a reduced gas flow in the combustion chamber, which was shown to lead to reduced engine heat transfer. However, the combination of the appropriate geometry, swirl level and combustion phasing was found to be decisive for the amount of heat lost through the engine walls.

All of the above mentioned results demonstrates how complex the engine operation is, with many interacting physical phenomena making up the behavior of an engine. By changing one part of the system, all other parts will be affected and the entire performance of the engine is changed. This is also true when it comes to heat transfer, as small changes in inlet conditions of the air can have large effects on how much heat is generated by combustion and then lost through wall heat transfer. In this work, it has been shown that for an effective control of heat losses, a combination of engine geometry, injection strategy and optimal heat release timings is required. At the same time, combustion temperature must be controlled to avoid unwanted emission production during the process. This optimum combination is going to be case dependent, in a sense that heavy duty engines and light duty engines will not have the same optimum solution. This highlights the need for further research in the field, both with engine test and simulation work.

Including gas exchange as well as the conjugate heat transfer from gas to coolant is essential in representing the entire cycle of the engine. This would be the next natural step for further heat transfer studies of diesel and PPC engines, with the goal of increasing the engine efficiency. Reducing heat losses by itself does not guarantee an improved engine efficiency, as the remaining energy must be converted to mechanical work in order to increase the efficiency. Therefore, the entire cycle, including the gas-exchange and cooling circuits, should be considered in future work.

As for the simulation of reactive flows in engines, the use of large eddy simulations could be beneficial for specific applications. In light-duty engines the spray-wall interaction is, in general, stronger that for heavy-duty engines. In these cases, the instantaneous fluctuations of the spray can be decisive in the

estimation of wall heat fluxes, as the location of the spray impingement on the piston wall can vary with the fluctuations. For this type of detailed resolution, LES is more beneficial than RANS, because of the nature of the two modeling types. Furthermore, information on spray fluctuations and air-entrainment in a fuel spray can be more accurately captured by LES, resulting in a more accurate representation of the combustion event. This information would also be of importance to further heat transfer predictions.

The presence of the thermal boundary layer tends to be problematic for simulation tools, which do not perform integration to the wall. Then, heat transfer estimations are dependent on the quality of the wall functions used. Most of the available wall functions make use of some sort of simplifications to the one-dimensional energy equation within the boundary layer. This would be an interesting topic to investigate, to aid future heat transfer predictions within complex domains, such as internal combustion engines.

Constructing a set of semi-empirical correlations for the convective heat transfer coefficient would be beneficial for the low temperature combustion concepts, as these correlations are frequently used in both heat release analysis of experimental data and in one-dimensional system simulations. Attempts have been made to construct these kind of correlations for, primarily, HCCI engines, but the correlations of Hohenberg and Woschni are still being used by many researchers.

On a more general note, increasing the efficiency of a combustion engine is a difficult task, where each percentage point increase in efficiency requires a huge effort. The knowledge acquired from this thesis work is a step in the direction of increased engine efficiency, but there is still a lot of work to be done in order to achieve the efficiency levels needed for the sustainable use of IC engines. This will require the combined effort of computer aided simulations, of all scales, and laboratory work with both single- and multi-cylinder engine tests.

Bibliography

[1] Swedish Energy Agency. Energy in Sweden, 2012. Annual report.

[2] DieselNet. Emission Standards (Downloaded October 2013), 2013. http://www.dieselnet.com/standards/.

[3] J.B. Heywood. *Internal Combustion Engine Fundamentals*. McGraw-Hill, New York, NY, 1988.

[4] G. Borman and K. Nishiwaki. Internal-combustion engine heat transfer. *Progress in Energy and Combustion Science*, 13(1):1–46, 1987.

[5] C. Arcoumanis, P. Cutter, and D. S. Whitelaw. Heat Transfer Processes in Diesel Engines. *Chemical Engineering Research & Design*, 76(2):124–132, 1998.

[6] J.K. Dukowicz. Quasi-Steady Droplet Phase Change in the Presence of Convection. Technical report, Los Alamos Scientific Lab., NM (USA), 1979.

[7] S. Sazhin, P. Krutitskii, W. Abdelghaffar, E. Sazhina, S. Mikhalovsky, S. Meikle, and M. Heikal. Transient heating of diesel fuel droplets. *International Journal of Heat and Mass Transfer*, 47:3327–3340, 2004.

[8] K. Nishiwaki. Modeling Engine Heat Transfer and Flame-Wall Interaction. *JSME*, pages 35–44, 1998. The Fourth International Symposium on Diagnostics and Modeling of Combustion in Internal Combustion Engines, COMODIA 98.

[9] Y. Cengel and M. Boles. *Thermodynamics: An Engineering Approach Sixth Edition (SI Units)*. McGraw-Hill, 2007.

[10] J. Dec. A Conceptual Model of DI Diesel Combustion Based on Laser-Sheet Imaging. *SAE Technical Paper 970873*, 1997. doi:10.4271/970873.

[11] T. Kamimoto and M.H. Bae. High Combustion Temperature for the Reduction of Particulate in Diesel Engines. *SAE Technical Paper 880423*, 1988.

[12] S. Onishi, S.H. Jo, K. Shoda, P. Do Jo, and S. Kato. Active Thermo-Atmosphere Combustion (ATAC) – A New Combustion Process for Internal Combustion Engines. *SAE Technical Paper 790501*, 1979.

[13] M. Christensen. *HCCI Combustion - Engine Operation and Emission Characteristics*. PhD Thesis, Lund University, Lund, Sweden, 2002. ISBN 91-628-5424-0.

[14] T. Johanson. *Turbucharged HCCI Engine - Improving Efficiency and Operating Range*. PhD Thesis, Lund University, Lund, Sweden, 2010. ISBN 987-91-7473-061-6.

[15] V. Manente. *Gasoline Partially Premixed Combustion; An Advanced Internal Combustion Engine Concept Aimed to High Efficiency, Low Emissions and Low Acoustic Noise in the Whole Load Range*. PhD Thesis, Lund University, Lund, Sweden, 2010. ISBN 987-91-628-8144-3.

[16] V. Manente, B. Johansson, P. Tunestal, C-G. Zander, and W. Cannella. An Advanced Internal Combustion Engine Concept for Low Emissions and High Efficiency from Idle to Max Load Using Gasoline Partially-Premixed Combustion. *SAE Technical Paper 2010-01-2198*, 2010.

[17] M. Shen, M. Tuner, B. Johansson, and W. Cannella. Effects of EGR and Intake Pressure on PPC of Conventional Diesel, Gasoline and Ethanol in a Heavy Duty Diesel Engine. *SAE Technical Paper 2013-01-2702*, 2013.

[18] M. Shen, M. Tuner, and B. Johansson. Close to Stoichiometric Partially Premixed Combustion -The Benefit of Ethanol in Comparison to Conventional Fuels. *SAE Technical Paper 2013-01-0277*, 2013.

[19] H. Fridriksson, B. Sundén, S Hajireza, and M. Tunér. CFD Investigation of Heat Transfer in a Diesel Engine with Diesel and PPC Combustion Modes. *SAE Technical Paper 2011-01-1838*, 2011.

[20] H. Fridriksson, S. Hajireza, M. Tunér, and B. Sundén. A CFD Investigation of Heat Transfer in a Diesel fueled PPC Engine Applying Design of Experiments. In *Proceedings of the 2012 ASME International Combustion Engine Divsision Fall Technical Conference, ICEF2012-92059*, Vancouver, BC, Canada, September 23-26 2012.

[21] H. Fridriksson, S. Hajireza, M. Tunér, and B. Sundén. CFD Investigation on Injection Strategy and Gasoline Quality Impact on In-Cylinder Temperature Distribution. *SAE Technical Paper 2013-24-0009*, 2013.

[22] M. Lundgren, M. Tuner, B. Johansson, S. Bjerkborn, K. Frojd, A. Andersson, F. Mauss, and B. Jiang. Gasoline PPC: A Parametric Study of Late Cycle Mixing Conditions using a Predictive Two-zone SRM Modeling Tool. *SAE Technical Paper 2013-01-2621*, 2013.

[23] M. Tuner. Potential ESC Performance of a Multi-Cylinder Heavy Duty PPC Truck Engine: System Simulations based on Single Cylinder Experiments. *SAE Technical Paper 2013-01-0268*, 2013.

[24] M. Tuner, B. Johansson, P. Keller, and M. Becker. Loss Analysis of a HD-PPC Engine with Two-Stage Turbocharging Operating in the European Stationary Cycle. *SAE Technical Paper 2013-01-2700*, 2013.

[25] D.A. Splitter, R.M. Hanson, S.L. Kokjohn, and R. D. Reitz. Improving Engine Performance by Optimizing Fuel Reactivity with a Dual Fuel PCCI Strategy. *THIESEL 2010 Conference on Thermo- and Fluid Dynamic Processes in Diesel Engines, Valencia, Spain*, 2010.

[26] S. Kokjohn, R. Hanson, D. Splitter, and R.D. Reitz. Experiments and Modeling of Dual-Fuel HCCI and PCCI Combustion Using In-Cylinder Fuel Blending. *SAE Technical Paper 2009-01-2647*, 2009.

[27] S.L. Kokjohn, R.M. Hanson, D.A. Splitter, and R.D. Reitz. Fuel reactivity controlled compression ignition (RCCI): a pathway to controlled high-efficiency clean combustion. *International Journal of Engine Research*, 12:209–226, 2011.

[28] R. Hanson and R.D. Reitz. Transient RCCI Operation in a Light-Duty Multi-Cylinder Engine. *SAE International Journal of Engines*, 6:1694–1705, 2013.

[29] D. Splitter, R. Hanson, S. Kokjohn, and R. Reitz. Reactivity Controlled Compression Ignition (RCCI) Heavy-Duty Engine Operation at Mid-and High-Loads with Conventional and Alternative Fuels. *SAE Technical Paper 2011-01-0363*, 2011.

[30] M. Musculus, P.C. Miles, and L.M. Pickett. Conceptual models for partially premixed low-temperature diesel combustion. *Progress in Energy and Combustion Science*, 39(2-3):246 – 283, 2013.

[31] W Nusselt. *Der Wärmeübergang in der Verbrennungskraftmaschine*, volume 67. Verlag d. Vereines deutscher Ingenieure, 1923.

[32] G. Eichelberg. Some new investigations on old combustion engine problems. *Engineering*, 148(27):463–466, 1939.

[33] W. Annand and T. Ma. Instantaneous Heat Transfer Rates to the Cylinder Head Surface of a Small Compression-Ignition Engine. *Proceedings of the Institution of Mechanical Engineers*, 185:976–987, 1970.

[34] G Woschni. A universally applicable equation for the instantaneous heat transfer coefficient in the internal combustion engine. *SAE International*, (64):3065–3083, 1967. SAE Paper 670931.

[35] G.F. Hohenberg. Advanced Approaches for Heat Transfer Calculations. *SAE Transactions*, 88:61–77, 1979. SAE paper 790825.

[36] A. Sharief. Study on Heat Transfer Correlation in IC Enginges. *SAE International*, 01(1816), 2008. 2008-01-1816.

[37] J. Galindo, J.M. Luján, J.R. Serrano, V. Dolz, and S. Guilain. Description of a heat transfer model suitable to calculate transient processes of turbocharged diesel engines with one-dimensional gas-dynamic codes. *Applied Thermal Engineering*, 26(1):66–76, 2006.

[38] C. Depcik and D. Assanis. A Universal Heat Transfer Correlation for Intake and Exhaust Flows in a Spark-Ignition Internal Combustion Engine. *SAE International*, 111(3):734–740, 2002.

[39] J. Chang, O. Güralp, Z. Filipi, D. Assanis, T. W. Kuo, P. Najt, and R. Rask. New Heat Transfer Correlation for an HCCI Engine Derived from Measurements of Instantaneous Surface Heat Flux. *SAE Technical Paper 2004-01-2996*, 2004.

[40] H.S. Soyhan, H. Yasar, H. Walmsley, B. Head, G.T. Kalghatgi, and C. Sorusbay. Evaluation of heat transfer correlations for {HCCI} engine modeling. *Applied Thermal Engineering*, 29(2–3):541 – 549, 2009.

[41] Q Xin. Theoretical Analysis of Internal Combustion Engine Miscellaneous Heat Losses. *SAE Technical Paper 2009-01-2881*, 2009.

[42] R.T. Green, K. Jambunathan, and S.D. Probert. Heat Transfers Through Diesel-Engine Cylinder Liners. *Applied Energy*, 14(3):175 – 196, 1983.

[43] V.P. Singh, P.C. Upadhyay, and N.K. Samria. Some Heat Transfer Studies on a Diesel Engine Piston. *International Journal of Heat and Mass Transfer*, 29(5):812–814, 1986.

[44] R. Prasad and NK Samria. Investigation of Heat Transfer in an Oil Cooled Piston With and Without Ceramic Insulation on Crown Face. *International Journal of Mechanical Sciences*, 31(10):765–777, 1989.

[45] C.D. Rakopoulos and G.C. Mavropoulos. Components Heat Transfer Studies in a Low Heat Rejection DI Diesel Engine Using a Hybrid Thermostructural Finite Element Model. *Applied Thermal Engineering*, 18(5):301–316, 1998.

[46] E. Urip, K. H. Liew, S. L. Yang, and O. Arici. Numerical Investigation of Heat Conduction with Unsteady Thermal Boundary Conditions for Internal Combustion Engine Application. *ASME Paper IMECE2004-59860*, 2004. ASME International Mechanical Engineering Congress and RD&D Expo, November.

[47] E. Urip. Modeling IC Engine Conjugate Heat Transfer Using the KIVA Code. *Numerical Heat Transfer, Part A: Applications*, 52(1):1–23, 2007.

[48] R.D. Reitz and C.J. Rutland. Development and Testing of Diesel Engine CFD Models. *Progress Energy Combustion Science*, 21:173–196, 1995.

[49] C.D. Rakopoulos, G.M. Kosmadakis, and E.G. Pariotis. Critical evaluation of current heat transfer models used in CFD in-cylinder engine simulations and establishment of a comprehensive wall-function formulation. *Applied Energy*, 87(5):1612—1630, 2010. doi:10.1016/j.apenergy.2009.09.029.

[50] M. Nuutinen, O. Kaario, and M. Larmi. Conjugate Heat Transfer in CI Engine CFD Simulations. *SAE Technical Paper 2008-01-0973*, 2008.

[51] F. Dong, Q. Fan, Y. Cai, S. Jiang, C. Guo, W. Norihiko, and W. Lee. Numerical Simulation of Boiling Heat Transfer in Water Jacket of DI Engine. *SAE Technical Paper 2010-01-0262*, 2010.

[52] Y. Li and S-C. Kong. Coupling conjugate heat transfer with in-cylinder combustion modeling for engine simulation. *International Journal of Heat and Mass Transfer*, 54(11–12):2467 – 2478, 2011.

[53] S. Fontanesi, G. Cicalese, A. D'Adamo, and G. Pivetti. Validation of a CFD Methodology for the Analysis of Conjugate Heat Transfer in a High Performance SI Engine. *SAE Technical Paper 2011-24-0132*, 2011. doi:10.4271/2011-24-0132.

[54] S. Fontanesi and M. Giacopini. Multiphase CFD-CHT optimization of the cooling jacket and FEM analysis of the engine head of a V6 diesel engine. *Applied Thermal Engineering*, 52(2):293 – 303, 2013.

[55] S Hajireza. Application of CFD Modeling in Combustion Bowl Assessment of Diesel Engines Using DoE Methodology. *SAE Technical Paper 2006-01-3330*, 2006.

[56] S.B. Pope. *Turbulent flows*. Cambridge University Press, 2000.

[57] H.K. Versteeg and W. Malalasekera. *An Introduction to Computational Fluid Dynamics: The Finite Volume Method*. Longman Group, 1995.

[58] P.R. Spalart. Strategies for turbulence modelling and simulations. *International Journal of Heat and Fluid Flow*, 21(3):252–263, 2000.

[59] K. Hanjalic, M. Popovac, and M. Hadziabdic. A robust near-wall elliptic-relaxation eddy-viscosity turbulence model for CFD. *International Journal of Heat and Fluid Flow*, 25(6):1047–1051, 2004.

[60] P.A. Durbin. Near-wall turbulence closure modeling without 'damping functions'. *Theoretical and Computational Fluid Dynamics*, 3(1):1–13, 1991.

[61] M. Popovac and K. Hanjalic. A combined WF and ItWF treatment of wall boundary conditions for turbulent convective heat transfer. In *9th UK National Heat Transfer Conference, Manchester, UK*, 2005.

[62] M. Popovac and K. Hanjalic. Compound wall treatment for RANS computation of complex turbulent flows and heat transfer. *Flow, Turbulence and Combustion*, 78(2):177–202, 2007.

[63] H. Lehtiniemi. *Development of Transient Flamelet Library Based Combustion Models*. PhD Thesis, Lund University, Lund, Sweden, 2013. ISBN 978-91-7473-507-9.

[64] B.F. Magnussen and B.H. Hjertager. On mathematical modeling of turbulent combustion with special emphasis on soot formation and combustion. In *Symposium (International) on Combustion*, volume 16, pages 719–729. Elsevier, 1977.

[65] B. Jayashankara and V. Ganesan. Effect of fuel injection timing and intake pressure on the performance of a DI diesel engine - A parametric study using CFD. *Energy Conversion and Management*, 51:1835–1848, 2010.

[66] S. Kong, Z. Han, and R.D. Reitz. The development and application of a diesel ignition and combustion model for multidimensional engine simulation. *SAE Technical Paper 950278*, 1995.

[67] O. Colin and A. Benkenida. The 3-zones extended coherent flame model (ECFM3Z) for computing premixed/diffusion combustion. *Oil & Gas Science and Technology*, 59(6):593–609, 2004.

[68] S.R. Turns. *An Introduction to Combustion: Concepts and Applications*. McGraw-Hill International Editions, 2000.

[69] J. Farrell, N. Cernansky, F. Dryer, C. Law, D.G. Friend, C. A. Hergart, R. M. McDavid, A. K. Patel, C. J. Mueller, and H. Pitsch. Development of an Experimental Database and Kinetic Models for Surrogate Diesel Fuels. *SAE Technical Paper 2007-01-0201*, 2007.

[70] J.C. Guibet and E. Faure-Birchem. *Fuels and Engines: Technology, Energy, Environment, Volume 1*. Editions Technip, Paris, 1999.

[71] M. Mehl, W.J Pitz, C.K. Westbrook, and H.J. Curran. Kinetic Modeling of Gasoline Surrogate Components and Mixtures Under Engine Conditions. *Proceedings of the Combustion Institute*, 33:193–200, 2011.

[72] M. Mehl, W. J. Pitz, M. Sjöberg, and J. E. Dec. Detailed kinetic modeling of low-temperature heat release for PRF fuels in an HCCI engine. *SAE Technical Paper 2009-01-1806*, 2009.

[73] H. J. Curran, P. Gaffuri, W. J. Pitz, and C.K. Westbrook. A Comprehensive Modeling Study of n-Heptane Oxidation. *Combustion and Flame*, 114:149–177, 1998.

[74] T. Tsurushima. A new skeletal PRF kinetic model for HCCI combustion. *Proceedings of the Combustion Institute*, 32:2835–2841, 2009.

[75] A. Patel, S. Kong, and R. Reitz. Development and Validation of a Reduced Reaction Mechanism for HCCI Engine Simulations. *SAE Technical Paper 2004-01-0558*, 2004. doi:10.4271/2004-01-0558.

[76] L. Liang, J.G. Stevens, and J.T. Farrell. A dynamic multi-zone partitioning scheme for solving detailed chemical kinetics in reactive flow computations. *Combustion Science and Technology*, 181(11):1345–1371, 2009.

[77] J. Xi and B. Zhong. Soot in diesel combustion systems. *Chemical engineering & technology*, 29(6):665–673, 2006.

[78] F. Tao, S. Srinivas, R.D. Reitz, and D.E. Foster. Comparison of Three Soot Models Applied to Multi-Dimensional Diesel Combustion Simulations. *JSME International Journal Series B Fluids and Thermal Engineering*, 48(4):671–678, 2005.

[79] F. Mauss and M. Balthasar. Simplification of a Detailed Kinetic Soot Model for Application in 3-D Programs. *Energy, Combustion and the Environment*, 4:7–10, 1997. Combustion Technologies for a Clean Environment.

[80] G. Agafonov, M. Nullmeier, P. Vlasov, J. Warnatz, and I. Zaslonko. Kinetic modeling of solid carbon particle formation and thermal decomposition during carbon suboxide pyrolysis behind shock waves. *Combustion Science and Technology*, 174(5-6), 2002.

[81] J. Appel, H. Bockhorn, and M. Frenklach. Kinetic Modeling of Soot Formation with Detailed Chemistry and Physics: Laminar Premixed Flames of C2 Hydrocarbons. *Combustion and Flame*, 121(1-2):122–136, 2000.

[82] A. Evlampiev, S. Frolov, V. Basevich, and A. Belyaev. *Chemical Physics Reports*, 20(1):21–27, 2001.

[83] J. Kiefer, S. Sidhu, R. Kern, and K. Xie. The Homogeneous Pyrolysis of Acetylene II: The High Temperature Radical Chain Mechanism. *Combustion Science and Technology*, 82:101–130, 1992.

[84] A. Krestinin. Detailed Modeling of Soot Formation in Hydrocarbon Pyrolysis. *Combustion and Flame*, 121:513–524, 2000.

[85] H. Wagner, P. Vlasov, K. Dorge, A. Eremin, I. Zaslonko, and D. Tanke. The Kinetics of Carbon Cluster Formation during C3O2 Pyrolysis. *Kinetics and Catalysis*, 42(5):645–656, 2001.

[86] H. Wang and M. Frenklach. A Detailed Kinetic Modeling Study of Aromatics Formation in Laminar Premixed Acetylene and Ethylene Flames. *Combustion and Flame*, 110(1-2):173–221, 1997.

[87] M. Costa, U. Sorge, and Allocca L. CFD optimization for GDI spray model tuning and enhancement of engine performance. *Advances in Engineering Software*, 49:43–53, 2012.

[88] E. Loth. Numerical approaches for motion of dispersed particles, droplets and bubbles. *Progress in Energy and Combustion Science*, 26(3):161 – 223, 2000.

[89] J.K. Dukowicz. A particle-fluid numerical model for liquid sprays. *Journal of Computational Physics*, 35(2):229 – 253, 1980.

[90] R.D. Reitz. Modeling Atomization Process in High-Pressure Vaporizing Sprays. *Journal of Atomization Spray Technology*, 3:309–337, 1987.

[91] B.E. Launder and D.B. Spalding. The Numerical Computation of Turbulent Flows. *Computer Methods in Applied Mechanics and Engineering*, 3(2):269 – 289, 1974.

[92] C. Angelberger, T. Poinsot, and B. Delhaye. Improving Near-Wall Combustion and Wall Heat Transfer Modeling in SI Engine Computations. *SAE Technical Paper 972881*, 1997.

[93] Z. Han and R.D. Reitz. A Temperature Wall Function Formulation for Variable-Density Turbulent Flows with Application to Engine Convective Heat Transfer Modeling. *International Journal of Heat and Mass Transfer*, 40(3):613–625, 1997.

[94] M. Nuutinen, O. Kaario, and M. Larmi. Advances in Variable Density Wall Functions for Turbulent Flow CFD-Simulations, Emphasis on Heat Transfer. *SAE Technical Paper 2009-01-1975*, 2009.

[95] V. Manente, B. Johansson, P. Tunestal, and W. Cannella. Effects of Different Fuel Types on Heavy Duty Partially Premixed Combustion. *SAE Technical Paper 2009-01-2668*, 2009.

[96] H. Fridriksson, B. Sundén, and S. Hajireza. A theoretical study on the heat transfer process in diesel engines. *Advanced Computational Methods and Experiments in Heat Transfer XI, (Eds. B Sundén, U. Mander, C.A. Brebbia)*, pages 177–188, 2010. WIT Press, UK.

[97] Ö. Andersson, J. Somhorts, R. Lindgren, R. Blom, and M. Ljungqvist. Development of the Euro 5 Combustion System for Volvo Cars' 2.4 l Diesel Engine. *SAE Technical Paper 2009-01-1450*, 2009.

[98] J. Styron, B. Baldwin, B. Fulton, D. Ives, and S. Ramanathan. Ford 2011 6.7L Power Stroke Diesel Engine Combustion System Development, 2011.

[99] T. Hashizume, S. Ishiyama, T. Ogawa, T. Tomoda, M. Kono, and K. Inagaki. Low Cooling Heat Loss and High Efficiency Diesel Combustion using

Restricted In-Cylinder Flow. In *The Eighth International Conference on Modeling and Diagnostics for Advanced Engine Systems (COMODIA 2012)*, 2012.

[100] H. Fridriksson, M. Tuner, Ö. Andersson, B. Sundén, H. Persson, and M. Ljungqvist. Effect of Piston Bowl Shape and Swirl Ratio on Engine Heat Transfer in a Light-Duty Diesel Engine. *Submitted to the SAE World Congress, Detroit, USA*, 2014.